

The 2-Channel Kondo Model II: CFT Calculation of Non-Equilibrium Conductance through a Nanoconstriction containing 2-Channel Kondo Impurities

Jan von Delft^{1,*}, A. W. W. Ludwig², Vinay Ambegaokar¹

¹*Laboratory of Atomic and Solid State Physics, Cornell University, Ithaca, NY 14853, USA*

² *University of California, Santa Barbara, CA 93106 , USA*

(February 4, 1996)

Abstract

Recent experiments by Ralph and Buhrman on zero-bias anomalies in quenched Cu nanoconstrictions (reviewed in the preceding paper, I), are in accord with the assumption that the interaction between electrons and nearly degenerate two-level systems in the constriction can be described, for sufficiently small voltages and temperatures ($V, T < T_K$), by the 2-channel Kondo (2CK) model. Motivated by these experiments, we introduce a generalization of the 2CK model, which we call the nanoconstriction 2-channel Kondo model (NTKM), that takes into account the complications arising from the non-equilibrium electron distribution in the nanoconstriction. We calculate the conductance $G(V, T)$ of the constriction in the weakly non-equilibrium regime of $V, T \ll T_K$ by combining concepts from Hershfield's Y -operator formulation of non-equilibrium problems and Affleck and Ludwig's exact conformal field theory (CFT) solution of the 2CK problem (CFT technicalities are discussed in a subsequent paper, III). Finally, we extract from the conductance a universal scaling curve $\Gamma(v)$ and compare it with experiment. Combining our results with those of Hettler, Kroha and Hershfield, we conclude that the NTKM achieves quantitative agreement with the experimental data.

I. INTRODUCTION

This is the second in a series of three papers (I,II,III)^{1,2,3} devoted to the 2-channel Kondo model (2CK). In the preceding paper (I), we gave a detailed review of a possible experimental realization of this model, namely the experiments by Ralph and Buhrman (RB)^{4,5,6,7} on non-magnetic zero-bias anomalies (ZBAs) in Cu nanoconstrictions. The experimental facts were summarized in the form of nine important properties of the data, (P1) to (P9) (see section IV of I). The main conclusion of paper I was that all experimental facts are in accord with the assumption that the ZBA is caused by the scattering of electrons off nearly degenerate two-level systems (TLS), with whom they interact according to the non-magnetic Kondo model of Zawadowski^{8,9}, which renormalizes to the 2CK model at sufficiently low temperatures. (See Appendices B and C for background on Zawadowski's model.)

In the present paper (II), we focus on property (P6): in the so-called *weakly non-equilibrium regime* of sufficiently small voltages and temperatures ($V < V_K$ and $T < T_K$, where V_K and T_K are experimentally determined cross-over scales, but arbitrary ratio $v = eV/k_B T$) the conductance $G(V, T)$ was found to satisfy the following scaling relation⁶:

$$\frac{G(V, T) - G(0, T)}{T^\alpha} = F(v) , \quad (1)$$

with scaling exponent $\alpha = \frac{1}{2}$. This was interpreted as strong evidence that the samples fall in the low-temperature regime of the 2CK model, because its conformal field theory (CFT) solution by Affleck and Ludwig (AL)^{10,11} suggests precisely such a scaling form near its $T = 0$ fixed point, and correctly predicts that $\alpha = \frac{1}{2}$, as observed.

If this interpretation is correct, it would imply that RB had directly observed non-Fermi-liquid behavior, because in the 2CK model, the exponent $\alpha = \frac{1}{2}$ is one of the signatures of non-Fermi-liquid physics (for a Fermi liquid, $\alpha = 2$). Thus RB's experiments attracted a lot of interest, because non-Fermi-liquid behavior, so treasured by theorists, has been very difficult to demonstrate experimentally.

However, it is of course quite conceivable that the scaling behavior can also be accounted for by some other theory. Indeed, Wingreen, Altshuler and Meir^{12,(a)} have pointed out that an exponent of $\alpha = \frac{1}{2}$ also arises within an alternative interpretation of the experiment, based not on 2CK physics but the physics of disorder (which we believe, though, to contradict other important experimental facts, see section V A of I).

It is therefore desirable to develop additional quantitative criteria for comparing the experiment to various theories. Now, in paper I it was shown that a sample-independent scaling function $\Gamma(v)$ could be extracted from the sample-dependent scaling function $F(v)$ of Eq. (1). According to the 2CK interpretation, this $\Gamma(v)$ should be a universal scaling function, a fingerprint of the 2CK fixed point, independent of sample-specific details. A very stringent quantitative test of any theory for the RB experiment would therefore be to calculate $\Gamma(v)$, and compare it to experiment.

The present paper is devoted to this task. $\Gamma(v)$ is calculated analytically within the framework of the 2CK model and its exact CFT solution by AL, and the results are compared to the RB experiment. When combined with recent numerical results of Hettler, Kroha and Hershfield *et al.*¹³, agreement with the experimental scaling curve is obtained, thus lending further quantitative support to the 2CK interpretation for the Cu constrictions.

In order to describe the scattering of electrons off two-level systems *in a nanoconstriction geometry*, we introduce a generalization of the 2CK model, which we call the *nanonconstriction two-channel Kondo model (NTKM)*, that takes into account the complications arising from the non-equilibrium electron distribution in the nanoconstriction. The generalization consists of labelling the electrons by an additional *species* index $\sigma = (L, R)$, which denotes their direction of incidence (toward the left or right for electrons injected from the right or left lead).

In equilibrium ($V = 0$), our NTKM reduces to the 2CK. Therefore, for $T \ll T_K$, it displays the same non-Fermi-liquid behavior as the latter. When the voltage is turned on, by continuity *there must exist a regime in which the voltage is still sufficiently small (namely $V \ll T_K$) that non-Fermi-liquid behavior persists despite $V \neq 0$* . We shall call this $T, V \ll T_K$ regime the *non-Fermi-liquid regime*, and associate it with the scaling regime of (P6) identified in the experiment. At higher voltages ($V \gtrsim T_K$), the non-Fermi-liquid behavior is destroyed. Therefore, we shall focus exclusively on the case $V \ll T_K$ in this paper, and accordingly the acronym NTKM will henceforth be understood to stand for “the nanonconstriction 2-channel Kondo model in the non-Fermi-liquid regime”.

The non-Fermi-liquid regime has to be treated by non-perturbative methods. The method we use combines ideas from CFT with concepts from Hershfield’s Y -operator formulation of non-equilibrium problems¹⁴. We show that all one needs to calculate the current using Hershfield’s formalism are certain scattering amplitudes, to be denoted by $\tilde{U}_{\eta\eta'}(\varepsilon')$. We assume that in the non-Fermi-liquid regime, the scattering amplitudes are essentially independent of V (since V -dependent corrections are of order $V/T_K \ll 1$ and hence negligible (they are discussed in Appendix I)). We then show that the $V = 0$ values of the scattering amplitudes can be extracted from an equilibrium Green’s function $G_{\eta\eta'}(\tau, ix; \tau', ix') = -\langle T\psi_\eta(\tau, ix)\psi_{\eta'}^\dagger(x') \rangle$ that is known exactly from CFT.

Once they are known, it is straightforward to calculate the non-linear current $I(V, T)$ through the constriction, and extract from it the scaling function $\Gamma(v)$.

The present paper can be read without knowledge of CFT, because the only step for which CFT is really needed, namely the calculation of $G_{\eta\eta'}$, is carried out in paper III, and here we only cite the needed results.

The outline of this paper is as follows: In section II we introduce the NTKM, and in section III outline our strategy for solving it by a combination of CFT methods with Hershfield’s Y -operator approach. This strategy is implemented in section IV, where the scattering states are calculated. The current and scaling function are calculated in section V. Our results for $\Gamma(v)$ are compared to experiment and the NCA results of Hettler, Kroha and Hershfield in section VI, and our conclusions summarized in section VII.

More than half of the paper is taken up by appendices. The lengthier ones (A,B,C,D,F,H) summarize, for the sake of convenience, background material that is assumed known in the main text; the others (E,V,I) contain original work related to the main text. In appendix A, we recall some standard results from the semi-classical theory of non-equilibrium transport through a ballistic nanoconstriction. Appendices B and C provide a brief review of the recent series of papers by Zaránd and Zawadowski on the (bulk) non-magnetic Kondo model and its renormalization toward the 2CK model at low temperatures. Recent criticism of their conclusions are discussed in Appendix D. In Appendix E we compare our CFT results with those from the poor man’s scaling approach in the limit of large number ($k \rightarrow \infty$), in which

the latter approach becomes exact. Hershfield's Y -operator formalism is briefly reviewed in appendix F. Appendix G illustrates the general formalism developed in sections IV and V with a simple example. In appendix H we give some background on the NCA calculations of Hettler, Kroha and Hershfield. Finally, in appendix I we discuss V/T_K -correction to our results.

II. THE NANOCONSTRICITION NON-MAGNETIC KONDO MODEL

In this section we introduce a new model, to be called the *nanoconstriction two-channel Kondo model* (NTKM), to describe the interaction of conduction with a TLS in the nanoconstriction. We shall take as guideline the results of Zawadowski and coworkers, who introduced the non-magnetic Kondo Hamiltonian to describe the TLS-electron interaction (summarized in Appendix B) and showed that under renormalization it flows towards the non-Fermi-liquid fixed point of the 2CK model (in a way summarized in Appendix C).¹ However, we shall not be interested in the details of the renormalization process from some bare to some effective model. Instead our attitude, stated in section XB 2 of I, is that of phenomenologists: since the detailed microscopic nature of the presumed TLSs is unknown, so too is the “correct” microscopic, bare Hamiltonian. The best one can hope for is to find a phenomenological Hamiltonian that satisfactorily accounts for the observed phenomena. As argued at length in paper I, the 2CK model with energy splitting $\Delta \simeq 0$ passes this test on a qualitative level. We regard this as sufficient justification to use 2CK ideas as a basis for quantitative calculations, in order to test whether quantitative agreement with experiment can be achieved.

The NTKM that we shall write down is the simplest model we can think of that contains the non-Fermi-liquid physics of the 2CK model, but also accounts for the complications brought about by a nanoconstriction geometry relative to the bulk situation. We introduce it as a phenomenological Ansatz, without attempting to provide a detailed microscopic derivation. Since our aim is to calculate a *universal* curve, characteristic of the 2CK model but experimentally found to be sample-independent, we believe that such lack of attention to microscopic details has experimental justification.

The main complications arising in a nanoconstriction geometry relative to the bulk case are, firstly, that one has to distinguish between electrons leaving and entering the L and R leads, and secondly, that the application of a voltage induces a non-equilibrium electron distribution in the nanoconstriction.

We thus have to deal with a non-equilibrium problem with non-trivial interactions. The standard procedure (due to Kadanoff and Baym¹⁸) for defining such a problem requires

¹It should be pointed out that the question as to whether a realistic TLS-electron system will reach the 2CK non-Fermi-liquid regime under renormalization is currently controversial^{15,12,16,17} (see appendix D). In the present paper, though, we do not attempt to clarify any of the controversial issues. We simply take the view that it would be useful to know what the scaling curve looked like if the system indeed does reach the 2CK non-Fermi-liquid regime, and hence do the calculation, assuming it does.

conceptual care and may for clarity be organized into six steps:

First the problem is defined in the absence of interactions, by defining

- (S1) a free Hamiltonian H_o with eigenstates $\{|\varepsilon\eta\rangle_o\}$,
- (S2) a free density matrix ρ_o governing their non-equilibrium occupation,
- (S3) and the physical quantities of interest, in our case the current I (with expectation value $\langle I \rangle = \text{Tr}\rho_o I / \text{Tr}\rho_o$ in the absence of interactions).

Then the interactions are switched on, by defining

- (S4) an interaction Hamiltonian H_{int} ,
- (S5) and the full density matrix ρ , which governs their non-equilibrium occupation of states for the fully interacting system. (Typically, this is done by adiabatically switching on H_{int} , and keeping track of how the initial ρ_o develops into a final ρ .)
- (S6) Expectation values are calculated according to $\langle I \rangle = \text{Tr}\rho I / \text{Tr}\rho$.

In this section, we address steps (S1) to (S4). [(S5) and (S6) are discussed in sections IV V, respectively]. We also explain, within the poor man's scaling approach, why the flow towards the non-Fermi-liquid regime is not disrupted by $V \neq 0$ as long as $V \ll T_K$.

A. Free Hamiltonian H_o

We consider a single TLS at the center of the nanoconstriction (see Fig. 1 of paper I for a sketch of the nanoconstrictions used in the RB experiment). We consider only those modes of electrons that contribute to the ZBA, i.e. that interact with this TLS when passing through the nanoconstriction.

To describe these electrons, we imagine that the “free nanoconstriction Schrödinger equation” for free electrons and some random static impurities but no TLS-electron interaction, with boundary conditions that all electron wave-functions vanish on the metal-insulator boundary, has already been solved (impossible in practice, but not in principle). This provides us [step (S1)] with a complete set of single-particle eigenstates $\{|\varepsilon, \eta\rangle_o = c_{o\varepsilon\eta}^\dagger |0\rangle\}$ (where $|0\rangle$ = vacuum), in terms of which H_o is diagonal:

$$H_o = \sum_{\eta} \int_{-D}^D d\varepsilon \varepsilon c_{o\varepsilon\eta}^\dagger c_{o\varepsilon\eta}. \quad (2)$$

Here the continuous energy label ε is taken to lie in a band of width $2D$, symmetric about the equilibrium Fermi energy (at $\varepsilon = 0$), with constant² density of states³ N_o . The latter

²Very recent work by Zaránd and Udvárdi¹⁹ has shown that using a constant density of states is probably less realistic in a nanoconstriction than in the bulk (where it is standard), because the local density of states fluctuates strongly as a function of r and ε . This is the kind of complication that our phenomenological approach has to ignore.

³Since the density of states diverges for infinite systems, the expectation values of some operators, e.g. the current [e.g. see footnote 5 and Eq. (39)], have to be evaluated in a finite system with a discrete energy spectrum. In such cases, we use the replacement rules: $\int d\varepsilon \longrightarrow N_o^{-1} \sum_{\varepsilon}$, and $\delta(\varepsilon - \varepsilon') \longrightarrow N_o \delta_{\varepsilon\varepsilon'}$.

has been absorbed into the normalization of the $c_{o\varepsilon\eta}^\dagger$'s, which we take as

$$\{c_{o\varepsilon\eta}, c_{o\varepsilon\eta}^\dagger\} = \delta_{\eta\eta'}\delta(\varepsilon - \varepsilon') . \quad (3)$$

The label η collectively denotes a set of discrete quantum numbers, $\eta \equiv (\sigma, \alpha, i) = (\text{species}, \text{pseudo-spin}, \text{channel})$ -index, which have the following meaning: $i = \uparrow, \downarrow$ is the electron's Pauli spin, which will be seen below to play the role of *channel*-index in the NTKM. $\alpha = 1, 2$ is a discrete *pseudo-spin index*, the nanoconstriction analogue of Vladár and Zawadowski's "angular" index α [see e.g. Eq.(2.36) of the first paper of⁹; in¹³, α was called a "parity" index]. It labels those two sets of free states $\{|\varepsilon, \sigma, 1, i\rangle\}$ and $\{|\varepsilon, \sigma, 2, i\rangle\}$ that in the non-Fermi-liquid regime will couple most strongly to the TLS. For example, if the free wave-functions were expanded in terms of angular harmonics, $\alpha = 1, 2$ would label two complicated linear combinations of $Y_{l,m}(\theta, \phi)$ functions. Strictly speaking α can take on a large number of discrete values, but we ignore all but two, in the spirit of Zawadowski's bulk result⁹ that the others decouple when the temperature is lowered and the system flows toward a non-Fermi-liquid fixed point with an effective electron pseudo-spin of $\frac{1}{2}$. (The modes we ignore contribute to the background conductance, but not to the ZBA.)

Finally, $\sigma = (+, -) = (L, R)$, the *species index*, denotes the direction of propagation of the incident electron: $\sigma = L = +$ for left-moving electrons, incident toward the left from $z = +\infty$ in the right lead; $\sigma = R = -$ for right-moving electrons, incident toward the right from $z = -\infty$ in the left lead. (For example, in spherical coordinates the asymptotic behavior of the incident (or transmitted) parts of the wave-function of both L - and R -movers will be proportional to e^{-ikr}/r (or e^{ikr}/r) as $r \rightarrow \infty$.) The nanoconstriction geometry necessitates this distinction between L - and R -movers (not needed in the bulk case), firstly because L - and R -movers originate from different leads, which are at different chemical potentials if $V \neq 0$, and secondly because they contribute with different sign to the current.

B. The free density matrix ρ_o

We now turn to step (S2), the definition of ρ_o , the free density matrix for $H_{int} = 0$ but arbitrary voltage. The right and left leads have chemical potentials (measured relative to the equilibrium chemical potential μ) of $+eV/2$ and $-eV/2$, respectively.⁴ As input, we use a standard result from the semi-classical theory of non-equilibrium transport of electrons through a ballistic nanoconstriction²⁰ (summarized in appendix A): At the center of the constriction, the distribution of occupied electron states in momentum space is highly anisotropic (see Fig. 2 of Appendix A). It consists of *two* sectors, to be denoted by L or R , that contain the momenta of all electrons that are *incident as L or R -movers*, i.e. are injected from the R or L leads. Consequently, the Fermi energies of the L/R sectors are equal to those of the R/L leads, namely $\mu_{\pm} = \pm\frac{1}{2}eV$.

⁴Our figures and arguments are given for the case $eV > 0$. We take $e = -|e|$ and hence $V = -|V|$. With $\mu_{\pm} = \pm eV/2$ for R/L leads, there then is a net flow of electrons from right to left, and the current to the right is positive.

We formalize these standard results by associating the L/R sectors with the *species* quantum number $\sigma = L/R = \pm$ introduced above (correspondingly μ_η will stand for μ_\pm), and adopting the following form for the free density matrix ρ_o :

$$\rho_o \equiv e^{-\beta[H_o - Y_o]} , \quad \langle O \rangle_o \equiv \frac{\text{Tr} \rho_o O}{\text{Tr} \rho_o} , \quad (4)$$

where the Y_o -operator is defined by

$$Y_o \equiv \frac{1}{2}eV(N_L - N_R) = \sum_\eta \mu_\eta \int d\varepsilon c_{o\varepsilon\eta}^\dagger c_{o\varepsilon\eta} . \quad (5)$$

Here N_L and N_R denote the total number of L - and R -moving electrons.⁵ It follows that

$$\langle c_{o\varepsilon\eta}^\dagger(\tau) c_{o\varepsilon'\eta'}(\tau') \rangle = e^{\varepsilon(\tau-\tau')} f(\varepsilon, \eta) \delta_{\eta\eta'} \delta(\varepsilon - \varepsilon') , \quad \text{where } f(\varepsilon, \eta) \equiv \frac{1}{e^{\beta(\varepsilon-\mu_\eta)} + 1} . \quad (6)$$

C. The free current through the nanoconstriction

The ZBA arises from backscattering by the TLS of electrons that would otherwise have passed through the constriction. Thus, we assume that they would contribute one unit e^2/h of conductance if the interaction were turned off. (More generally, one could use $\mathcal{T}_\eta e^2/h$, where \mathcal{T}_η is a transmission coefficient, but this only affects the (non-universal) amplitude of the ZBA.) Thus, we may define [step (S3)] our current operator simply as the difference between the number of electrons transmitted as L - or R -movers:

$$\hat{I} = \frac{|e|}{N_o h} \sum_\eta \int d\varepsilon \sigma c_{o\varepsilon\eta}^\dagger c_{o\varepsilon\eta} . \quad (7)$$

Our signs are chosen such that $\langle \hat{I} \rangle_o > 0$ if the net flow of electrons is from right to left, while the prefactor $|e|/hN_o$ is needed, because of our choice of normalization, to obtain⁵ a conductance of e^2/h per channel.

D. The nanoconstriction 2CK interaction

We now come to step (S4), the specification of the electron-TLS interaction, for which we make the following phenomenological Ansatz:

$$H_{int} = \int d\varepsilon \int d\varepsilon' \sum_{\eta\eta'} c_{o\varepsilon\eta}^\dagger V_{\eta\eta'} c_{o\varepsilon'\eta'} , \quad V_{\eta\eta'} \equiv v_K v_{\sigma\sigma'} \delta_{ii'} \left(\frac{1}{2} \vec{\sigma}_{\alpha\alpha'} \cdot \vec{S} \right) , \quad (8)$$

⁵To evaluate $\langle c_{o\varepsilon\eta}^\dagger c_{o\varepsilon\eta} \rangle$ we have to give meaning to $\delta(\varepsilon - \varepsilon)$ of Eq. (6), which seems to diverge because we took the thermodynamic limit of an infinitely large system. We do this by replacing it by the corresponding finite-system expression of $N_o \delta_{\varepsilon\varepsilon'}$ [see footnote 3], i.e. we use $\langle c_{o\varepsilon\eta}^\dagger c_{o\varepsilon\eta} \rangle = f(\varepsilon, \eta) N_o$.

Here \vec{S} is the TLS pseudo-spin operator acting in the two-dimensional Hilbert space of the TLS. Following the assumption (A2) of section VID of I, we henceforth assume that Δ , the TLS excitation energy, is the smallest energy scale in the problem, and set $\Delta = 0$.

As far as the pseudospin and channel indices α and i are concerned, H_{int} is simply the isotropic 2CK Hamiltonian to which, according to Zawadowski's analysis for a bulk system, a realistic TLS coupled to electrons will flow at sufficiently low temperatures. However, we introduced an extra Hermitian 2×2 matrix $v_{\sigma\sigma'}$, which enables an incident electron, say a L -mover, to be scattered into either a L - or a R -mover, independent of whether its pseudo-spin index α and that of the TLS do or do not flip.⁶ In general, $v_{\sigma\sigma'}$ can be any Hermitian matrix, but, for reasons given below, it is actually sufficient to consider only the very simple case

$$v_{\sigma\sigma'} = \frac{1}{2} \begin{pmatrix} 1 & 1 \\ 1 & 1 \end{pmatrix}_{\sigma\sigma'} . \quad (9)$$

Note that with this choice, our model is equivalent (after a Schrieffer-Wolf transformation) to a model recently studied by Hettler *et. al.* using numerical NCA techniques, with whose results we shall compare our own (see section VIB).

The Hamiltonian introduced above is strictly speaking not a 2CK Hamiltonian, since $\sigma = \pm$ and $i = \uparrow, \downarrow$ give *four* different combinations of indices that do not Kondo-couple to the impurity. However, the it can be mapped onto a 2-channel model by making a unitary transformation,

$$\bar{c}_{o\varepsilon\bar{\eta}} = N_{\bar{\eta}\eta} c_{o\varepsilon\eta} , \quad N_{\bar{\eta}\eta} \equiv N_{\bar{\sigma}\sigma} \delta_{\bar{\alpha}\alpha} \delta_{ii} , \quad (10)$$

chosen such that it diagonalizes $v_{\sigma\sigma'}$. For our present choice (9) for $v_{\sigma\sigma'}$, $N_{\bar{\sigma}\sigma}$ is given by

$$N_{\bar{\sigma}\sigma} = \frac{1}{\sqrt{2}} \begin{pmatrix} 1 & 1 \\ 1 & -1 \end{pmatrix}_{\bar{\sigma}\sigma} , \quad (NvN^{-1})_{\bar{\sigma}\bar{\sigma}'} = \begin{pmatrix} 1 & 0 \\ 0 & 0 \end{pmatrix}_{\bar{\sigma}\bar{\sigma}'} . \quad (11)$$

We shall refer to the operators $c_{o\varepsilon\eta}$ as *L/R* operators and the $\bar{c}_{o\varepsilon\bar{\eta}}$ as *even/odd* operators, and always put a bar over all indices and matrices referring to the even/odd basis. In the even-odd basis, the interaction becomes

$$H_{int} = \int d\varepsilon \int d\varepsilon' \sum_{\bar{\eta}, \bar{\eta}'} \bar{c}_{o\varepsilon\bar{\eta}}^\dagger \bar{c}_{o\varepsilon'\bar{\eta}'} \bar{V}_{\bar{\eta}\bar{\eta}'} , \quad \bar{V}_{\bar{\eta}\bar{\eta}'} = v_K \delta_{ii'} \begin{pmatrix} \frac{1}{2} \vec{\sigma}_{\bar{\alpha}\bar{\alpha}'} \cdot \vec{S} & 0 \\ 0 & 0 \end{pmatrix}_{\bar{\sigma}\bar{\sigma}'} . \quad (12)$$

Thus, in the even/odd basis, one set of channels, the *odd channels* ($\bar{\sigma} = o$), completely decouples from the impurity. The other set of channels, the *even channels* ($\bar{\sigma} = e$), constitute a true 2CK problem, which will eventually be responsible for the non-Fermi liquid behavior of the NTKM.

⁶ Note that the interaction of Eqs. (8) and (9) is reminiscent of the tunneling Hamiltonian H_{tun} in the standard problem of electrons tunneling through an insulating barrier that separates two electronic baths: the off-diagonal components of $v_{\sigma\sigma'}$ transfers an electron from one bath to the other, with the implicit assumption that this does not disturb the thermal distribution of electrons significantly.

If one chooses a more general $v_{\sigma\sigma'}$ than Eq. (9), the odd channel will not completely decouple, but (barring some accidental degeneracies) the even and odd channels will always couple to the TLS with different strengths. At low enough temperatures, the one coupled more weakly can be assumed to decouple completely (à la Zawadowski⁹, see section C3 of Appendix B), leaving again a 2CK problem for the even channel. This is the reason why it is sufficient to take $v_{\sigma\sigma'}$ as in (9).

E. Poor Man's Scaling Equations unaffected by V

The model we wrote down assumes that the NFL regime of the TLS-electron system has already been reached. However, one may wonder whether having $V \neq 0$ would not prevent the TLS-electron system from reaching the non-Fermi-liquid regime at all. That this is not the case for V sufficiently small ($\ll T_K$) can be seen by the following poor man's scaling argument: Since the poor man's scaling equations are derived by adjusting the cut-off from D to D' , which are both $\gg V, T$, they are independent of V for the same reason as that they are independent of T (namely the change in coupling constants needed to compensate $D \rightarrow D'$ does not depend on energies V and T that are much smaller than D). In other words, the scaling equations for $V \neq 0$ are the same as those for $V = 0$, meaning that the initial RG flow is unaffected by $V \neq 0$. Eventually, the RG flow is cut off by either V or T , whichever is larger; however, if both are $\ll T_K$, the RG flow will terminate in the close vicinity of the non-Fermi-liquid fixed point, even if $V \neq 0$. This is the basis of our key assumption, stated in the introduction and implicit in the Ansatz (8), that for $V/T_K \ll 1$ the non-Fermi-liquid regime is governed by essentially the same effective Hamiltonian as for $V = 0$.

III. OUTLINE OF GENERAL STRATEGY

We now have to address step (S5) of the process of defining a fully interacting, non-equilibrium problem, namely the definition of the full density matrix ρ for $V \neq 0$ and $H_{int} \neq 0$. In this section, the heart of this paper, we propose a strategy for doing this which combines ideas from CFT with Hershfield's Y -operator formulation of non-equilibrium problems. The section is conceptual in nature; technical details follow in sections IV and V, and in paper III.

A. Hershfield's Y -operator approach to Non-Equilibrium Problems

Typically, the full ρ is defined by adiabatically turning on H_{int} and following the evolution of the initial density matrix ρ_o to a final ρ (see appendix F). Expanding the time-evolution operator in powers of H_{int} , one then generates a perturbation expansion that can be handled using the Keldysh technique.

However, for the Kondo problem, perturbation theory breaks down for $T < T_K$, where many-body effects become important. Therefore we shall adopt Hershfield's so-called Y -operator formulation of non-equilibrium problems¹⁴, which is in principle non-perturbative.

The main idea of Hershfield's approach (briefly summarized in appendix III A), is as follows. As the interaction H_{int} is adiabatically turned on, the density operator adiabatically evolves from its initial form $\rho_o = e^{-\beta(H_o - Y_o)}$ into a final form that Hershfield writes as $\rho \equiv e^{-\beta(H - Y)}$. This defines the operator Y , which is the adiabatically evolved version of Y_o and is conserved ($[Y, H] = 0$). The formal similarity between ρ and ρ_o implies that in terms of the non-equilibrium scattering states, the non-equilibrium problem has been cast in a form that is formally equivalent to an equilibrium problem.

This becomes particularly evident if one considers the set of simultaneous eigenstates of H and Y , which we shall call the *scattering states* and denote by $\{|\varepsilon\eta\rangle = c_{\varepsilon\eta}^\dagger |0\rangle\}$. Loosely speaking, they can be viewed as the states into which the free basis states $\{|\varepsilon\eta\rangle_o\}$ develop as H_{int} is turned on (in the sense that $c_{\varepsilon\eta}^\dagger$ is some function of the $\{c_{o\varepsilon'\eta'}^\dagger\}$, which reduces to $c_{o\varepsilon\eta}^\dagger$ for $H_{int} = 0$). For scattering problems like the NTKM, in which a free electron is incident upon a scatterer and scatters into something complicated, there evidently must be a one-to-one correspondence between the states $|\varepsilon\eta\rangle_o$ and $|\varepsilon\eta\rangle$: the incident parts of their wave-functions $\langle \vec{x}|\varepsilon\eta\rangle_o$ and $\langle \vec{x}|\varepsilon\eta\rangle$ must be identical. (The outgoing parts, which contain scattering information, will of course be different – this will be made explicit in Eq. (34) below.) This is why the free and scattering states can be labelled by the same indices, and also have the same density of states.⁷

Furthermore, for such scattering problems, H and Y will have the following form:⁸

$$H = \sum_\eta \int d\varepsilon \varepsilon c_{\varepsilon\eta}^\dagger c_{\varepsilon\eta} , \quad (13)$$

$$Y \equiv \sum_\eta \int d\varepsilon \mu_\eta c_{\varepsilon\eta}^\dagger c_{\varepsilon\eta} \quad (\neq Y_o) . \quad (14)$$

The form used here for Y here follows because Y evolves from Y_o as H_{int} is turned on, implying that Y can be obtained from Y_o by *replacing* the $c_{o\varepsilon\eta}$ in Eq. (5) by the scattering-state operators $c_{\varepsilon\eta}$ into which the latter evolve¹⁴. Eq. (13) and (14) imply that non-equilibrium thermal expectation values of the $c_{\varepsilon\eta}$'s have the standard form:

$$\langle c_{\varepsilon\eta}^\dagger(\tau) c_{\varepsilon'\eta'}(\tau') \rangle = e^{\varepsilon(\tau-\tau')} f(\varepsilon, \eta) \delta_{\eta\eta'} \delta(\varepsilon - \varepsilon') \quad \text{where} \quad f(\varepsilon, \eta) \equiv \frac{1}{e^{\beta(\varepsilon - \mu_\eta)} + 1} . \quad (15)$$

This is precisely the same form as that satisfied by the non-interacting $c_{o\varepsilon\eta}$'s in the absence of interactions [see Eq. (6)]. The intuitive reason for this remarkably simple result is clear: *the Boltzmann weight of a scattering state must be the same as that of the corresponding free state, since the thermal equilibration that leads to the Boltzmann factors happens deep inside*

⁷One might ask whether the very notion of scattering states make sense for a dynamical impurity problem, since the scatterer is constantly flipping its pseudo-spin. However, in the CFT solution of Kondo problems, the impurity completely disappears from the scene (being absorbed in the definition of a new spin current, see Eq. (14) of paper III). Thus the theory contains only electron degrees of freedom, for which one *can* meaningfully introduce scattering states.

⁸For problems other than scattering problems, Eq. (14) does not necessarily hold.

the leads, before the electrons are injected and scattered by H_{int} (this of course remains true when L - and R leads have different chemical potentials – all that happens for $V \neq 0$ is that the occupation probabilities pick up a V -dependence reflecting from which lead the electron was injected).

This result provides us with a very clear picture of how the current through a nanoconstriction should be calculated: when injecting electrons from the leads into the constriction, the thermal weighting is done *precisely* as for free particles, i.e. an electron incident in the state $|\varepsilon'\eta'\rangle_o$ is injected with weight $f(\varepsilon', \eta')$. For each such electron, one has to determine the *scattering amplitude* $\tilde{U}_{\eta\eta'}(\varepsilon')$, i.e. the amplitude with which it emerges from the scattering process in the state $|\varepsilon', \eta\rangle_o$ (where we assumed elastic scattering). These amplitudes (defined more explicitly below, see section IV C) are the non-trivial ingredients of the scattering states, which contain all relevant information about the scattering process.⁹ Once they are known, it is straightforward to calculate the current as a thermally weighted sum over transmission probabilities.

Since expectation values expressed in terms of scattering states are so simple, it is useful to reexpress all physical operators in terms of them. To this end, we define $U_{\eta'\eta}(\varepsilon', \varepsilon) \equiv {}_o\langle \varepsilon'\eta' | \varepsilon\eta \rangle$ to be the unitary transformation that relates the scattering states to the free basis states:

$$|\varepsilon\eta\rangle = \sum_{\eta'} \int d\varepsilon' |\varepsilon'\eta'\rangle_o U_{\eta'\eta}(\varepsilon', \varepsilon) , \quad (16)$$

$$c_{\varepsilon\eta} = \sum_{\eta'} \int d\varepsilon' U_{\eta\eta'}^\dagger(\varepsilon, \varepsilon') c_{o\varepsilon'\eta'} ; \quad (17)$$

$$\delta_{\eta\eta'} \delta(\varepsilon - \varepsilon') = \sum_{\tilde{\eta}} \int d\tilde{\varepsilon} U_{\eta\tilde{\eta}}^\dagger(\varepsilon, \tilde{\varepsilon}) U_{\tilde{\eta}\eta'}(\tilde{\varepsilon}, \varepsilon') . \quad (18)$$

For example, the current of Eq. (7) takes the form:

$$I = \frac{|e|}{N_o h} \sum_{\eta\eta''} \int d\varepsilon \int d\varepsilon' \int d\varepsilon'' \text{Re} \left[\sigma U_{\eta'\eta}^\dagger(\varepsilon', \varepsilon) U_{\eta\eta''}(\varepsilon, \varepsilon'') \langle c_{\varepsilon'\eta'}^\dagger c_{\varepsilon''\eta''} \rangle \right] . \quad (19)$$

⁹ For a many-body problem such as the Kondo problem, complicated combinations of particle-hole excitations are created upon scattering, which can not simply be written as a linear combination $\sum_{\eta} c_{o\varepsilon'\eta}^\dagger \tilde{U}_{\eta\eta'}(\varepsilon')$ of single-particle excitations. However, it was shown by Maldacena and Ludwig²² that the scattering matrix for free electrons incident on a Kondo impurity is unitary if the single-particle Hilbert space of free-electron states $\{|\varepsilon\eta\rangle_o\}$ is appropriately enlarged to include “Kondo excitations” (see section III and appendix III of paper III). This means that the outgoing states can be written as linear combinations of free-electron states $\{|\varepsilon\eta\rangle_o\}$ and a new set of Kondo excitation states $\{|\varepsilon\eta\rangle_{\tilde{o}}\}$. The corresponding set of creation operators $\{\tilde{c}_{o\varepsilon\eta}^\dagger\}$ are complicated functions (not mere linear combinations) of the $\{c_{o\varepsilon'\eta}^\dagger\}$ and will be constructed explicitly in paper III. Thus, in the formalism developed below, the unitary transformation in Eq. (16) is implicitly understood to act in the enlarged Hilbert space of $\{|\varepsilon\eta\rangle_o, |\varepsilon\eta\rangle_{\tilde{o}}\}$ states, and the collective index η implicitly includes another index $a = (f, k)$ to distinguish free from Kondo states. However, this will only be made explicit in paper III.

The reality of I is of course automatically ensured by the hermiticity of the current operator, and the reminder $\text{Re}[\quad]$ has been inserted merely for future convenience.

We shall show below that the $U_{\eta\eta'}(\varepsilon, \varepsilon')$, and hence also the current, are completely determined by the $\tilde{U}_{\eta\eta'}(\varepsilon')$. Unfortunately, Hershfield's formalism gives no recipe for finding these explicitly for a given problem. Thus, the crucial question now becomes: how does one calculate the scattering amplitudes?

B. Equating CFT- and scattering-state Green's Functions

In general, finding the scattering amplitudes is just as difficult as solving the problem by other (e.g. Keldysh) methods. However, for $V = 0$ the even sector of the NTKM is equivalent to the 2CK model, which AL solved exactly using CFT^{23,24,25,26,10,27,11}. (This equivalence is shown explicitly below, when we rewrite the model in field theoretical language, see Eq. (27) and (28) below.) Therefore, we propose that the scattering states of the NTKM can be extracted from AL's results. We now explain how this can be done.

One of AL's central results is an explicit and exact expression for the equilibrium Green's $G_{\eta\eta'} = -\langle \psi_\eta \psi_{\eta'}^\dagger \rangle$ [defined explicitly in Eq. (29)], which gives the amplitude that an incident η' -electron will emerge from the scattering process as outgoing η -electron. Evidently, it must contain information about the scattering amplitudes. Indeed, we shall show that when the same equilibrium Green's function is calculated explicitly using the scattering state formalism, it is completely determined by $\tilde{U}_{\eta\eta'}(\varepsilon')$. Therefore, *by equating the scattering-states form for $G_{\eta\eta'}$ to the corresponding CFT result, $\tilde{U}_{\eta\eta'}(\varepsilon')$ can be extracted from the latter.*

Of course, this procedure only yields the $V = 0$ value of $\tilde{U}_{\eta\eta'}$, whereas to calculate the nonequilibrium current, we actually need its $V \neq 0$ values too. Moreover, it is clear that in general $\tilde{U}_{\eta\eta'}$ must depend on V , since if V is sufficiently large, it is known to non-trivially affect the many-body physics of the Kondo problem. For example, for $V \neq 0$, the difference in Fermi energies of the L - and R leads causes the Kondo peak in the density of states to split^{69,68} into two separate peaks (at energies $\mu \pm \frac{1}{2}eV$, see Fig. 9 of Appendix H, taken from³⁰). Moreover, the effective Hamiltonian in poor-man's scaling approaches depends on V if it is the largest low-energy cut-off in the problem (see section II E), and if V is too large, it will cut off the renormalization group flow towards the non-Fermi-liquid fixed point before non-Fermi-liquid regime is reached.

However, such V -induced effects should be negligible for sufficiently small V . For example, when $V \ll T_K$, the splitting of the Kondo peak by eV is negligible compared to its width, which is $\propto T_K$. Said in poor-man's scaling language, if $(T <) V \ll T_K$, then $V \neq 0$ cuts off the renormalization group flow at a point sufficiently close to the non-Fermi-liquid fixed point that the physics should still governed by the latter. Hence, we propose that in the non-Fermi-liquid regime of $V \ll T_K$, the V -dependence of the scattering amplitudes is negligible, and hence shall always use their $V = 0$ values below. (In a sense, the condition that this procedure be valid can be regarded as our definition of the “non-Fermi-liquid regime”.) More formally, we assume that $\tilde{U}_{\eta\eta'}$ can be expanded in powers of V/T_K , and use only the zeroth term. (In Appendix I, we show that the leading V/T_K correction only produces a subleading correction to the desired scaling function.)

The intuitive motivation for neglecting the V -dependence of the scattering amplitudes is based on the assumption that the effect of $V \neq 0$ can be characterized as follows if $V \ll T_K$: although the leads inject electrons into the non-Fermi-liquid state that, since ε_F , are able to probe its nature at energies different from ε_F , they only probe gently, i.e. they inject sufficiently few that the non-Fermi-liquid state itself is not disrupted. Since the “output” of this probing, namely the scattering amplitudes, depend non-linearly on ε , the current will depend non-linearly on V , too, even if $\tilde{U}_{\eta\eta'}(\varepsilon')$ itself is V -independent.

Another underlying assumption of our proposed strategy is that the strong-coupling or fixed-point fields $\psi_\eta(\tau, ix)$ occurring in the CFT treatment can be expanded in terms of a set of fermionic excitations, else it would not make sense to equate a CFT Green’s function to one constructed from scattering states. That this is indeed the case will be shown in paper III.

IV. EXTRACTING SCATTERING STATES FROM CFT RESULTS

To implement our strategy for finding $\tilde{U}_{\eta\eta'}$, the first step is to rewrite the NTKM of section II in field theory language by introducing a set of fields $\psi_\eta(ix)$. Then we define the Green’s function $G_{\eta\eta'} = -\langle T\psi_\eta\psi_{\eta'}^\dagger \rangle$, and show that it is completely determined by $\tilde{U}_{\eta\eta'}$ (which turns out to be its spectral function). Finally, we equate this $G_{\eta\eta'}$ to the corresponding exact CFT result of AL, which allows us to obtain the corresponding exact expression for $\tilde{U}_{\eta\eta'}$ explicitly.

A. Transcription to Field Theory

To rewrite the “bare” NTKM introduced in section II in field theory language, we introduce for each channel η a 1-dimensional, second-quantized field $\psi_\eta(\tau, ix)$ (with $x \in [-l, l]$, $l \rightarrow \infty$) as a Fourier-integral over all ε :¹⁰

$$\psi_\eta(ix) \equiv \frac{1}{\sqrt{\hbar v_F}} \int_{-\infty}^{\infty} d\varepsilon e^{-i\varepsilon x/\hbar v_F} c_{o\varepsilon\eta}, \quad (20)$$

$$c_{o\varepsilon\eta} = \frac{1}{\sqrt{\hbar v_F}} \lim_{l \rightarrow \infty} \int_{-l/2}^{l/2} \frac{dx}{2\pi} e^{i\varepsilon x/\hbar v_F} \psi_\eta(ix), \quad (21)$$

$$\{\psi_\eta(ix), \psi_{\eta'}^\dagger(ix)\} = 2\pi\delta_{\eta\eta'}\delta(x - x'). \quad (22)$$

The factors of \hbar and v_F , inserted for dimensional reasons, are henceforth set = 1.

Note that $\psi_\eta(ix)$ is *not* the usual electron field $\Psi(\vec{x})$, which is constructed from the actual (unknown) wave-functions $\langle \vec{x} | \varepsilon \eta \rangle_o$ through $\Psi(\vec{x}) \equiv \sum_\eta \int d\varepsilon \langle \vec{x} | \varepsilon \eta \rangle_o c_{o\varepsilon\eta}$. Instead, $\psi_\eta(ix)$ is best thought of simply as the Fourier transform of $c_{o\varepsilon\eta}$, this being a convenient way of rewriting

¹⁰Strictly speaking, the $\int d\varepsilon$ integrals have to be cut off, $\int_{-D}^D d\varepsilon$, at a bandwidth D satisfying $T, V \ll D$. However, we take $D \rightarrow \infty$ (since the errors thus introduced are of order $T/D, V/D \ll 1$ and hence negligible even for finite D). This allows us to invert relations such as (20) straightforwardly.

the problem in field-theoretical language. Nevertheless, the role of x is strongly analogous to that of the “radial” coordinate of the actual wave-function $\Psi_{\varepsilon\eta}(\vec{x})$, and $\psi_\eta^\dagger(x)$ can be interpreted as the operator that creates an electron with quantum numbers η at “position” x .

Using Eq. (21), H_o and H_{int} of Eqs. (2) and (8) can be written as

$$H_o = \sum_{\eta\eta'} \int_{-\infty}^{\infty} \frac{dx}{2\pi} \psi_\eta^\dagger(ix) i\partial_x \psi_\eta(ix) , \quad (23)$$

$$H_{int} \equiv \sum_{\eta\eta'} \psi_\eta^\dagger(0) V_{\eta\eta'} \psi_{\eta'}(0) . \quad (24)$$

By simple Fourier transformation, we have hence arrived at a 1+1-dimensional field theory, defined by Eqs. (23) and (24). The reason why this (and not a 3+1 dimensional theory) resulted, is essentially that there is only *one* continuous quantum number, namely ε , in the problem, with respect to which we can Fourier transform. This in turn is a result of the constriction geometry, which defines a definite and unique origin, and consequently a notion of a single “radial” coordinate (in spherical coordinates it is the radius r), to which our x roughly corresponds. Moreover, the fact that we assumed a constant density of states and hence a linear dispersion implies that the free fields are conformally invariant, which is the key property required for the subsequent application of AL’s CFT methods.

The Heisenberg equation of motion,

$$-\partial_\tau \psi_\eta(\tau, ix) = [\psi_\eta(\tau, ix), H_o + H_{int}] = (\delta_{\eta\eta'} i\partial_x + 2\pi\delta(x) V_{\eta\eta'}) \psi_{\eta'}(ix) . \quad (25)$$

shows that for all $x \neq 0$, the fields depend only on $\tau + ix$. [This is the reason for writing the argument of ψ_η as (ix) in Eq. (20), since the τ dependence of ψ_η can then simply be obtained by analytic continuation $(ix \rightarrow \tau + ix)$.] Consequently, *by construction*, all fields are “mathematical left-movers”, incident from $x = \infty$ and traveling toward $x = -\infty$. The effect of the scattering term H_{int} is to mix the different incident channels with each other at $x = 0$, so that $\psi_\eta(\tau, ix)$ will differ from a free field only for $x < 0$. Thus, *we have turned our problem into a one-dimensional scattering problem*, with *all* free fields incident from the right, and *all* scattered ones outgoing to the left. This is in exact analogy to AL’s treatment of the Kondo problem, which in fact was the motivation for introducing both physical L - and R -movers as “mathematical left-movers” in Eq. (20). Of course, the distinction between *physical* L - and R -movers is carried by the index $\sigma = L, R$, and L - R backscattering is described by the $\sigma \neq \sigma'$ terms in $V_{\eta\eta'}$.

B. Transformation to even-odd basis

As mentioned in section IID, the relation between the NTKM and the standard 2CK model is best understood in the even-odd basis (denoted by bars) of operators $\bar{c}_{o\bar{\varepsilon}\bar{\eta}} = N_{\bar{\eta}\eta} c_{o\varepsilon\eta}$ [see Eq. (10)]. Therefore, we define even-odd fields

$$\bar{\psi}_{\bar{\eta}}(ix) = N_{\bar{\eta}\eta} \psi_\eta(ix) , \quad (26)$$

normalized according to Eq. (22). In terms of these, H_o and H_{int} of Eqs. (23) and (24) are:

$$H_o = \sum_{\bar{\eta}} \int_{-\infty}^{\infty} \frac{dx}{2\pi} \bar{\psi}_{\bar{\eta}}^{\dagger}(ix) i\partial_x \bar{\psi}_{\bar{\eta}}(ix) , \quad (27)$$

$$H_{int} = \sum_{\bar{\sigma} \bar{\alpha} \bar{\alpha}' \bar{i}} \bar{\psi}_{\bar{\sigma} \bar{\alpha} \bar{i}}^{\dagger}(0) \left(v_K \delta_{\bar{\sigma} e} \frac{1}{2} \vec{\sigma}_{\bar{\alpha} \bar{\alpha}'} \cdot \vec{S} \right) \bar{\psi}_{\bar{\sigma} \bar{\alpha}' \bar{i}}(0) . \quad (28)$$

The odd channel ($\bar{\sigma} = o$) decouples from H_{int} . In the even channel ($\bar{\sigma} = e$), $H_o + H_{int}$ is precisely the “bare” Hamiltonian of the equilibrium 2CK model solved exactly by AL [see e.g.¹¹, Eq. (2.17)]. Therefore, the even channels will display non-Fermi-liquid behavior for $T, V \ll T_K$.

C. Definition of scattering amplitude $\tilde{U}_{\eta\eta'}(\varepsilon')$

Having rewritten the model in field theory language, we can define the equilibrium Green’s function that is to be the link to AL’s CFT results:¹¹

$$G_{\eta\eta'}(\tau, -ir; \tau', ir') \equiv -\langle T\psi_{\eta}(\tau, -ir)\psi_{\eta'}^{\dagger}(\tau', ir') \rangle , \quad \text{with } r, r' > 0 . \quad (29)$$

Since its arguments correspond to taking $x = -r < 0$ and $x' = r' > 0$, it gives the amplitude that an incident η' -electron will emerge from the scattering process as outgoing η -electron.

In order to calculate $G_{\eta\eta'}$ in terms of scattering states, we rewrite the fields $\psi_{\eta}(\tau, ix)$ (in the original L - R basis) in terms of the $c_{\varepsilon\eta}$ ’s. Inserting the inverse of Eq. (17) into Eq. (20) and defining

$$\phi_{\varepsilon'\eta'}(ix, \eta) \equiv \int d\varepsilon e^{-i\varepsilon x} U_{\eta\eta'}(\varepsilon, \varepsilon') , \quad (30)$$

we find

$$\psi_{\eta}(\tau, ix) = \sum_{\eta'} \int d\varepsilon' \phi_{\varepsilon'\eta'}(ix, \eta) c_{\varepsilon'\eta'}(\tau) , \quad (31)$$

which implies that $\phi_{\varepsilon'\eta'}(ix, \eta) = \langle \psi_{\eta}(\tau, ix) c_{\varepsilon'\eta'}^{\dagger}(\tau) \rangle$. Since by its definition (20) $\psi_{\eta}^{\dagger}(\tau, ix)$ has the interpretation of creating an electron with quantum numbers η at x , this shows that $\phi_{\varepsilon'\eta'}(ix, \eta)$ may be thought of as the “wave-function” for the scattering states $|\varepsilon'\eta'\rangle$.¹² It gives the amplitude for an electron in state $|\varepsilon'\eta'\rangle$ to be found at x with quantum number η . The orthonormality and completeness of these wave-functions is guaranteed by the unitarity (18) of $U_{\eta\eta'}(\varepsilon, \varepsilon')$:

$$\sum_{\bar{\eta}} \int \frac{d\tilde{x}}{2\pi} \phi_{\varepsilon\eta}^*(i\tilde{x}, \bar{\eta}) \phi_{\varepsilon'\eta'}(i\tilde{x}, \bar{\eta}) = \delta_{\eta\eta'} \delta(\varepsilon - \varepsilon') , \quad (32)$$

$$\sum_{\bar{\eta}} \int d\tilde{\varepsilon} \phi_{\varepsilon\bar{\eta}}^*(ix, \eta) \phi_{\varepsilon\bar{\eta}}(ix', \eta') = 2\pi \delta_{\eta\eta'} \delta(x - x') . \quad (33)$$

¹¹In paper III, this Green’s function is denoted by $G_{\eta\eta'}^{RL}(z^*; z')$, following the notation used AL.

¹²This interpretation of $\phi_{\varepsilon'\eta'}(ix, \eta)$ as a wave-function is meant as a mnemonic and should not be taken literally; as mentioned in section II A, the actual wave-functions are intractably complicated.

Now, because scattering takes place only at $x = 0$, for $x > 0$ (i.e. before the scatterer is encountered) the wave-function $\phi_{\varepsilon' \eta'}(ix, \eta)$ must correspond to the free wave-function $e^{-i\varepsilon' x}$ of the state $|\varepsilon' \eta'\rangle_o$. Thus, we make the following Ansatz:¹³

$$\phi_{\varepsilon' \eta'}(ix, \eta) \equiv e^{-i\varepsilon' x} \left[\tilde{U}_{\eta\eta'}(\varepsilon') \theta(-x) + \delta_{\eta\eta'} \theta(x) \right]. \quad (34)$$

This relation defines the matrix $\tilde{U}_{\eta\eta'}(\varepsilon')$, which clearly can be interpreted as a scattering amplitude, since it specifies the amplitude for an electron incident with quantum numbers $(\varepsilon' \eta')$ to emerge with quantum numbers $(\varepsilon' \eta)$.

The relation between the scattering amplitude $\tilde{U}_{\eta\eta'}(\varepsilon')$ and the matrix $U_{\eta\eta'}(\varepsilon, \varepsilon')$ can be found by inserting Eq. (34) into the inverse of Eq. (30):

$$U_{\eta\eta'}(\varepsilon, \varepsilon') = \int \frac{dx}{2\pi} e^{i\varepsilon x} \phi_{\varepsilon' \eta'}(ix, \eta) \quad (35)$$

$$= \frac{1}{2\pi i} \left[\frac{\tilde{U}_{\eta\eta'}(\varepsilon')}{\varepsilon - \varepsilon' - i\epsilon} - \frac{\delta_{\eta\eta'}}{\varepsilon - \varepsilon' + i\epsilon} \right] \quad (36)$$

($\epsilon > 0$ is infinitessimally small). This shows that $U_{\eta\eta'}(\varepsilon, \varepsilon')$ is completely known once $\tilde{U}_{\eta\eta'}(\varepsilon')$ is known. The unitarity condition Eq. (18) on $U_{\eta\eta'}(\varepsilon, \varepsilon')$ then immediately implies unitarity for $\tilde{U}_{\eta\eta'}(\varepsilon')$ (the $\int d\tilde{\varepsilon}$ integral can trivially be done by contour methods):

$$\sum_{\tilde{\eta}} \tilde{U}_{\eta\tilde{\eta}}(\varepsilon') \tilde{U}_{\tilde{\eta}\eta'}^\dagger(\varepsilon') \equiv \delta_{\eta\eta'} . \quad (37)$$

The unitarity of $\tilde{U}_{\eta\tilde{\eta}}(\varepsilon')$ could of course also have been anticipated from Eq. (34): it ensures that scattering conserves probability, i.e. that $\sum_{\eta} |\phi_{\varepsilon' \eta'}(ix, \eta)|^2$ is the same for $x > 0$ and $x < 0$.

The current can be rewritten as follows by inserting Eq. (36) into Eq. (19):

$$I = \frac{|e|}{N_o h} \sum_{\eta\eta'\eta''} \int d\varepsilon' \int d\varepsilon'' \text{Re} \left[\frac{\sigma}{2\pi i} \left(\frac{\tilde{U}_{\eta'\eta}^\dagger(\varepsilon') \tilde{U}_{\eta\eta''}(\varepsilon'')}{\varepsilon' - \varepsilon'' - 2i\epsilon} - \frac{\delta_{\eta'\eta} \delta_{\eta\eta''}}{\varepsilon' - \varepsilon'' + 2i\epsilon} \right) \langle c_{\varepsilon'\eta'}^\dagger c_{\varepsilon''\eta''} \rangle \right] \quad (38)$$

$$= \frac{|e|}{N_o h} \sum_{\eta\eta'\eta''} \int d\tilde{\varepsilon}' \int d\tilde{\varepsilon}'' \sigma \frac{1}{2} \left[\tilde{U}_{\eta'\eta}^\dagger(\varepsilon') \tilde{U}_{\eta\eta''}(\varepsilon'') + \delta_{\eta'\eta} \delta_{\eta\eta''} \right] \delta(\varepsilon - \varepsilon'') \langle c_{\varepsilon'\eta'}^\dagger c_{\varepsilon''\eta''} \rangle \quad (39)$$

$$= \frac{|e|}{h} \sum_{\eta'\eta} \int d\varepsilon' \sigma \frac{1}{2} \left[\tilde{U}_{\eta'\eta}^\dagger(\varepsilon') \tilde{U}_{\eta\eta'}(\varepsilon') + \delta_{\eta'\eta} \right] f(\varepsilon', \eta') . \quad (40)$$

To obtain Eq. (38), the $\int d\varepsilon$ integral in Eq. (19) was done using contour methods. Eq. (39) follows since the diagonal nature of $\langle c_{\varepsilon'\eta'}^\dagger c_{\varepsilon''\eta''} \rangle$ ensures that $U_{\eta'\eta}^\dagger(\varepsilon') U_{\eta\eta''}(\varepsilon'')$ is real, so that we may use $\text{Re}[(2\pi i)(\varepsilon' - \varepsilon'' \mp 2i\epsilon)]^{-1} = \pm \frac{1}{2} \delta(\varepsilon' - \varepsilon'')$. Finally, to obtain Eq. (40), we used footnote 5. The problem of calculating the current has thus been reduced to that of finding the scattering amplitude $\tilde{U}_{\eta\eta'}(\varepsilon)$.

¹³In writing Eq. (34), we have assumed elastic scattering ($\varepsilon_{in} = \varepsilon_{out}$). For a 2CK model, this holds only if the impurity energy splitting $\Delta = 0$, as assumed in this paper, so that electrons cannot exchange energy with the impurity.

D. Extracting $\tilde{U}_{\eta\eta'}$ from the Green's Function $G_{\eta\eta'}$

Using Eqs. (31), (34) and (15) (with $\mu' = 0$), $G_{\eta\eta'}$ of Eq. (29) can be reduced to the form

$$G_{\eta\eta'}(\tau, -ir; \tau', ir') = - \sum_{\tilde{\eta}\tilde{\eta}'} \int d\tilde{\varepsilon} d\tilde{\varepsilon}' \tilde{U}_{\eta\tilde{\eta}}(\tilde{\varepsilon}) \delta_{\tilde{\eta}'\eta'} \langle c_{\tilde{\varepsilon}\tilde{\eta}}(\tau) c_{\tilde{\varepsilon}'\tilde{\eta}'}^\dagger(\tau') \rangle e^{-i(-\tilde{\varepsilon}r - \tilde{\varepsilon}'r')} \quad (41)$$

$$= - \int d\tilde{\varepsilon} \tilde{U}_{\eta\eta'}(\tilde{\varepsilon}) \frac{e^{-\tilde{\varepsilon}(\tau - ir - \tau' - ir')}}{e^{-\beta\tilde{\varepsilon}} + 1} . \quad (42)$$

Its Matsubara-transform is readily found to be

$$G_{\eta\eta'}(i\omega_n; r, r') = \int d\varepsilon \frac{\tilde{U}_{\eta\eta'}(\varepsilon) e^{i\varepsilon(r+r')}}{i\omega_n - \varepsilon} , \quad (43)$$

This is the central result of this section: $G_{\eta\eta'}$ is completely determined by $\tilde{U}_{\eta\eta'}(\varepsilon)$, which is proportional to its spectral function. Conversely, by equating $G_{\eta\eta'}$ to the corresponding exact CFT result, $\tilde{U}_{\eta\eta'}(\varepsilon)$ can be extracted from the latter using

$$\tilde{U}_{\eta\eta'}(\varepsilon) = \frac{i}{2\pi} e^{-i\varepsilon(r+r')} \left[G_{\eta\eta'}(\varepsilon - \mu_{\eta'} + i0^+; r, r') - G_{\eta\eta'}(\varepsilon - \mu_{\eta'} - i0^+; r, r') \right] . \quad (44)$$

In the next section section, we cite the CFT results for $\bar{G}_{\bar{\eta}\bar{\eta}'}$ and $\tilde{\bar{U}}_{\bar{\eta}\bar{\eta}'}(\varepsilon)$ in the e/o basis, from which $G_{\eta\eta'}$ and $\tilde{U}_{\eta\eta'}(\varepsilon)$ can be obtained by

$$G_{\eta\eta'} = N_{\eta\bar{\eta}}^\dagger \bar{G}_{\bar{\eta}\bar{\eta}'} N_{\bar{\eta}'\eta'} , \quad \tilde{U}_{\eta\eta'}(\varepsilon) = N_{\eta\bar{\eta}}^\dagger \tilde{\bar{U}}_{\bar{\eta}\bar{\eta}'}(\varepsilon) N_{\bar{\eta}'\eta'} . \quad (45)$$

In appendix G the above formalism is illustrated by a simple example, namely potential scattering of two species of fermions (i.e. $\eta = 1, 2$).

E. Result of CFT calculation for $\bar{G}_{\bar{\eta}\bar{\eta}'}$ and $\tilde{\bar{U}}_{\bar{\eta}\bar{\eta}'}(\varepsilon)$

The CFT calculation of $\bar{G}_{\bar{\eta}\bar{\eta}'}$ and $\tilde{\bar{U}}_{\bar{\eta}\bar{\eta}'}(\varepsilon)$ in the e/o basis, which follows closely the work of AL, is outlined in section II D of III. For present purposes, it suffices to consider CFT as a “black box” that, starting from Eqs. (27) and (28), produces the following results.

$\tilde{\bar{U}}_{\bar{\eta}\bar{\eta}'}(\varepsilon)$ has the form

$$\tilde{\bar{U}}_{\bar{\eta}\bar{\eta}'}(\varepsilon) = \delta_{\bar{\alpha}\bar{\alpha}'} \delta_{\bar{\iota}\bar{\iota}'} \begin{pmatrix} \bar{U}^{(e)} & 0 \\ 0 & \bar{U}^{(o)} \end{pmatrix}_{\bar{\sigma}\bar{\sigma}'} , \quad (46)$$

$\bar{U}^{(e)}$ and $\bar{U}^{(o)}$ are the magnitudes of the scattering amplitudes in the even and odd channels, respectively. Since the odd channels decouple, $\bar{U}^{(o)} = 1$, for the even channels, $\bar{U}^{(e)}$ has the following scaling form (see Eq. (24) in paper III):

$$\bar{U}^{(e)}(\varepsilon, T) = \lambda T^{1/2} \tilde{\Gamma}(\varepsilon/T) e^{i\phi_e} . \quad (47)$$

Here $e^{i\phi_e}$ is a trivial phase shift¹⁴ that can occur in the Kondo channel if particle-hole symmetry is broken (see^{10, section IV}), and λ is a non-universal constant (called λ_7 in paper III). $\tilde{\Gamma}(x)$ is a universal scaling function, whose explicit form was calculated by AL¹⁰:

$$\tilde{\Gamma}(x) = \left\{ \frac{3}{2\sqrt{2}}(2\pi)^{1/2} 2 \sin(\pi/2) \int_0^1 du \left[u^{(-ix)/(2\pi)} u^{-1/2} (1-u)^{1/2} F(u) - \frac{\Gamma(2)}{\Gamma^2(3/2)} u^{-1/2} (1-u)^{-3/2} \right] \right\}. \quad (48)$$

$F(u) \equiv F(3/2, 3/2, 1; u)$ is a hypergeometric function. The $\int du$ integral can be done numerically for any value of x , thus giving us an explicit expression for the scaling function $\tilde{\Gamma}(x)$. The real and imaginary parts of $\tilde{\Gamma}(x) \equiv \tilde{\Gamma}_e(x) + i\tilde{\Gamma}_o(x)$ have the properties

$$\tilde{\Gamma}_{e/o}(x) = \pm \tilde{\Gamma}_{e/o}(-x), \quad \text{and} \quad \tilde{\Gamma}_e(x) < 0. \quad (49)$$

V. CALCULATION OF THE CURRENT AND SCALING FUNCTION

We now have all the ingredients for step (S6), the actual calculation of the current, from which we extract the desired scaling function $\Gamma(x)$.

1. Calculation of the current

Using Eq. (45) to express the current I of Eq. (40) in terms of the e/o scattering amplitude $\tilde{U}_{\bar{\eta}\eta'}(\varepsilon)$ of Eq. (46), we find:

$$I = \frac{|e|}{\hbar} \sum_{\eta'} \int d\varepsilon' \frac{1}{2} [P_{\eta'}(\varepsilon') + \sigma' T_{\eta'}] f(\varepsilon', \eta'), \quad (50)$$

$$P_{\eta'}(\varepsilon') \equiv \sum_{\eta} \left(N^\dagger \tilde{U}^\dagger N \right)_{\eta'\eta} \sigma T_{\eta} \left(N^\dagger \tilde{U} N \right)_{\eta\eta'}. \quad (51)$$

Let us now analyze the matrix product of Eq. (51) index by index. All matrices are diagonal in α, i , hence the sums $\sum_{\alpha i}$ in $P_{\eta'}$ are trivial. Next, consider matrix multiplication in the index σ . Using Eq. (11) for $N_{\bar{\sigma}\sigma}$, we find

$$P_{\eta'}(\varepsilon') = \sigma' \text{Re} \left(\tilde{U}^{\dagger(o)}(\varepsilon') \tilde{U}^{(e)}(\varepsilon') \right). \quad (52)$$

Note that in spite of the fact that the current operator is diagonal in η [see Eq. (7)], P_{η} turns out to have *o/e* cross terms, $\tilde{U}^{\dagger(o)} \tilde{U}^{(e)}$. This is a direct consequence of the *L-R* scattering

¹⁴We shall assume that the phase shift ϕ_e is energy-independent. In general, it can have an energy-dependence, $\phi_e = \phi_e^{(0)} + \frac{\varepsilon}{\varepsilon_F} \phi_e^{(1)} + \dots$, but this will be very weak (since $\varepsilon/\varepsilon_F$), and only give rise to subleading corrections in the conductance, i.e. terms of the form $(T^{3/2}/\varepsilon_F) \Gamma_{(1)}(V/T)$.

matrix $v_{\sigma\sigma'}$ introduced in Eq. (8): it necessitates the L/R -to- e/o basis transformation $N_{\sigma\sigma'}$ which produces a current operator that is off-diagonal in the e/o basis. The presence of o/e cross terms in $P_{\eta'}(\varepsilon')$ is extremely important, since $\overline{U}^{(e)}$, describing Kondo scattering in the even channel, has a $T^{1/2}$ contribution, but $\overline{U}^{(o)}$, describing no scattering at all in the odd channel, does not. Thus we see that our model contains a $T^{1/2}$ contribution to the current, as observed in experiment (compare property (P6) in paper I).

On the other hand, had we attempted to use a model without L/R scattering, i.e. with $v_{\sigma\sigma'} = \delta_{\sigma\sigma'}$ (such as the model studied by Schiller and Hershfield²⁹), no L/R -to- e/o basis transformation would have been needed; then $P_{\eta'}(\varepsilon')$ would be proportional to $\tilde{U}^\dagger \tilde{U}$, i.e. to $(T^{1/2})^2$, not $T^{1/2}$. Thus, the inclusion of L/R scattering into the model is absolutely essential to obtain the $T^{1/2}$ dependence.

In the above presentation, we glossed over one important subtlety: the scattering matrix $\tilde{U}_{\eta\eta'}$ must be unitary [see Eq. (37)], but the form given in Eq. (47) manifestly is not (since, e.g. $\overline{U}^{(e)} = 0$ for $T = 0$). This reflects the so-called “unitarity paradox”¹⁰, according to which the scattering matrix for free fermions off a 2-channel Kondo impurity into free fermions is not unitary, which seems to violate the conservation of probability during a scattering process. The resolution of this paradox²² is that the “missing probability” is scattered into a sector of Hilbert space that cannot be described in terms of linear combinations of *single-particle* fermionic excitations (compare footnote 9) but has a simple representation when the theory is bosonized. In paper III we shall discuss this issue in more detail, and show how to incorporate the resulting complications into the present framework. The upshot is that the expression (52) remains valid.

2. Calculation of scaling function $\Gamma(v)$

We now have gathered all the ingredients to derive the sought-after scaling form for the current and conductance. Inserting Eq. (52) into Eq. (50) gives

$$I = \frac{|e|}{h} 4 \int d\varepsilon' \frac{1}{2} \left\{ \text{Re} \left[\overline{U}^{(e)}(\varepsilon') \right] + 1 \right\} \left[f_o(\varepsilon' - eV/2) - f_o(\varepsilon' + eV/2) \right], \quad (53)$$

where the factor 4 comes from $\sum_{\alpha'i'}$ and the sum $\sum_{\sigma'}$, written out explicitly, gives the two terms in the last factor. Now, the conductance can be written in the form¹⁵

$$G = \left| \frac{\partial I}{\partial V} \right| = \frac{2e^2}{h} \int d\varepsilon' \left\{ \frac{1}{2} \text{Re} \left[\overline{U}^{(e)}(\varepsilon') \right] + \frac{1}{2} \text{Re} \left[\overline{U}^{(e)}(-\varepsilon') \right] + 1 \right\} (-\partial_\varepsilon f_o)(\varepsilon' - eV/2). \quad (54)$$

Thus, using Eq. (49) and (47), G reduces to

$$G = 2 \frac{e^2}{h} \left[1 - \lambda \gamma_o \cos \phi_e T^{1/2} \Gamma(\gamma_1 eV/T) \right]. \quad (55)$$

Here we introduced the universal scaling function $\Gamma(v)$, which is defined as follows in terms of the even part $\tilde{\Gamma}_e$ of the exactly known function $\tilde{\Gamma}$ of Eq. (48):

¹⁵To see this, use $(\partial_\varepsilon f_o)(\varepsilon' + eV/2) = (\partial_\varepsilon f_o)(-\varepsilon' - eV/2)$ and then change integration variables, $\varepsilon' \rightarrow -\varepsilon'$ in the second term of Eq. (53). Also recall the sign conventions of footnote 4.

$$\gamma_o \Gamma(\gamma_1 v) \equiv - \int dx \tilde{\Gamma}_e(x + v/2) [-\partial_x f_o(x)] , \quad (56)$$

where $v \equiv eV/T$, $x = \varepsilon'/T$, $f_o(x) = 1/(e^x + 1)$. The positive constants γ_o , γ_1 are to be chosen such that $\Gamma(v)$ obeys the normalization conditions [compare Eq. (13) of paper I]:

$$\Gamma(0) \equiv 1 , \quad \Gamma(v) \text{ vs. } v^{\frac{1}{2}} \text{ has slope } = 1 \text{ as } v^{\frac{1}{2}} \rightarrow \infty , \quad (57)$$

and a minus sign has been included in the definition (56) of Γ , since $\tilde{\Gamma}$ is negative definite [see Eq. (49)].

Thus, we have shown that within the present model, the conductance obeys the scaling relation¹⁶

$$G(V, T) = G_o + BT^{1/2} \Gamma(\gamma_1 v) , \quad (58)$$

with the universal scaling function $\Gamma(v)$, given by Eq. (56), known exactly. It is plotted as curve 6 in Fig. 6.

Note that this function is the same as that found in Eq. (20) of I (for $m = 1$ there) by a back-of-the-envelope calculation. The reason for this agreement is that $\tilde{\Gamma}_e(x)$ also turns out to determine the bulk scattering rate $\tau^{-1}(\varepsilon, T)$ through the relation

$$\lambda T^{1/2} \tilde{\Gamma}_e(\varepsilon, T) \propto 2\text{Im} \left(\Sigma^R(\varepsilon, T) - \text{Im} \Sigma^R(\varepsilon, 0) \right) = - \left(\tau^{-1}(\varepsilon, T) - \tau^{-1}(\varepsilon, 0) \right) , \quad (59)$$

where $\Sigma^R(\varepsilon, T)$ is the retarded bulk electron self-energy calculated by AL^{10,eq.(3.50)}. This *a posteriori* justifies the assumption made in section VII A 2 of I, namely that the nanoconstriction conductance will be governed by $\tau^{-1}(\varepsilon, T)$.

Note that according to the above calculation and Eq. (58), the slope of the scaling curve $[G(V, T) - G(0, T)]/BT^{1/2}$ seems to be universal, whereas in experiment it is not [see figure 11(a) of paper I]. The reason is that in our calculation we assumed that the impurity sits exactly at the center of the nanoconstriction, where the non-equilibrium between L - and R -movers is strongest, and hence feels the full effect of the applied voltage. However, as was explained in section III of paper I, an impurity not sitting exactly at the center of the constriction experiences an effective voltage $a_i V$, where the geometrical constant (of order unity) a_i depends on the position of the i -th impurity. When summing over all contributing impurities, one thus finds expression Eq. (22) of I, which is simply a sum of terms of the form (58), evaluated at slightly different voltages, corresponding to different impurity positions in the nanoconstriction. Our lack of knowledge about the a_i 's forces us to introduce another non-universal scaling factor A , and use the scaling form

$$G(V, T) = G_o + BT^{1/2} \Gamma(Av) , \quad (60)$$

¹⁶Note that consistency with the sign of the experimental zero-bias anomaly requires that $B = -2e^2/h\lambda\gamma_o \cos\phi_e$ must be > 0 , i.e. $\lambda \cos\phi_e < 0$. This is in agreement with AL^{10,p. 7309}, who concluded (for the case $\phi_e = 0$) that $\lambda < 0$ in the regime where the Kondo coupling constant is below its critical value, $\lambda_K < \lambda_K^*$, i.e. if one flows towards λ_K^* from the weak-coupling regime.

when comparing theory with experiment below (see Eq. (14) of paper I). When checking in the next section whether experimental (or numerical) data for $G(V, T)$ obeys this relation, we shall plot it in *maximally normalized* form (see section VII B 3 of paper I), i.e. we shall plot

$$\frac{G(V, T) - G(0, T)}{BT^{1/2}} \quad \text{vs.} \quad (Av)^{1/2}, \quad (61)$$

with A determined by the requirement that the asymptotic slope of the resulting function be equal to 1 [compare Eq. (57)]. According to Eq. (60), curves with different T should all collapse onto each other when plotted in this way, and the resulting curve should be identical to the universal curve $\Gamma(v) - 1$ vs. $v^{1/2}$.

3. Deviations from Scaling

It should be emphasized that the scaling relation found above is only expected to hold for $T/T_K \ll 1$, because it is based on keeping just the leading term in an expansion of $G_{\eta\eta'}$ in T/T_K . If T/T_K is not $\ll 1$, subleading powers of $(T/T_K)^{\alpha_n}$, that have been neglected in the calculation of $G_{\eta\eta'}$ will become important. They will give contributions of the form $(T/T_K)^{\alpha_n-1}\Gamma_n(v)$, which will cause further deviations from scaling.

Though it is possible in principle to calculate the functions $\Gamma_n(v)$ within our CFT approach, this would not be meaningful, because each additional subleading term that is added introduces a further non-universal, unknown constant λ_n . These constants would all have to be treated as fitting parameters, leading to more freedom than one would want for a meaningful comparison of theory and experiment.

VI. FINAL RESULT FOR SCALING CURVE

In this section we compare the CFT prediction of Eq. (56) for the universal scaling curve $\Gamma(v)$ to the experimental scaling curve of Fig. 11(b) of paper I. We also compare it to the results of Hettler, Kroha and Hershfield (HKH)^{13,30}, who used the non-crossing-approximation (NCA) technique for dealing with the Kondo problem.

A. A Few Words on the NCA Method

In order to understand what HKH did, a few introductory remarks about the NCA method and a summary of HKH's results are in order here. Some more details (including a comparison between the CFT and NCA results for the electron self-energy) may be found in appendix H.

HKH adopt an infinite- U Anderson Hamiltonian that can be mapped by a Schrieffer-Wolff transformation onto the NTKM [Eq. (8)] of Eqs. (27) and 28. The two models are therefore in the same universality class and describe the same low-energy physics.

HKH treat their model with the NCA technique, a self-consistent summation of an infinite set of selected diagrams, which they generalize to $V \neq 0$ using Keldysh techniques. The

NCA method is in a sense an uncontrolled approximation, since there is no small perturbation parameter, but for the 2-channel Kondo problem it turns out³¹ to give leading critical exponents for the impurity Green's function $A_d(\omega)$ in agreement with those obtained from conformal field theory. Hence the NCA method can be regarded as a useful interpolation between the high- T regime where any perturbative scheme works, and the low- T regime where it gives the correct exact critical exponents. Moreover, when combined with the Keldysh technique, it deals with the non-equilibrium aspects of the problem in a more direct way than our CFT approach, and is able to go beyond the weakly non-equilibrium regime.

Therefore, it is certainly meaningful to compare the NCA results of HKH to ours. CFT serves as a check on how well the NCA does at $V = 0$ and very low temperatures, where CFT is exact and NCA only an uncontrolled approximation. Conversely, if this check confirms the reliability of the NCA method in the low-energy regime, the latter can be used as a check on our use of CFT for $V \neq 0$ situations, where NCA presumably does the more reliable job.

HKH calculated the conductance $G(V, T)$ for a series of temperatures, measured in units of T_K , ranging from $T/T_K = 0.003$ to 0.5. Fig. 4(a) shows their results for $G(V, T)$, plotted according to Eq. (61) with $A = 1$ (i.e. without any adjustable parameters). The experimental data for sample #1 (which has $T_K \simeq 8K$) are shown for comparison in Fig. 4(b).

The lowest T/T_K values in Fig. 4(a) show good scaling, in accord with the CFT prediction. However, for larger T -values, marked deviations from scaling occur, just as seen in the experimental curves of Fig. 4(b). It is one of the strengths of the NCA method that deviations from scaling are automatically obtained, without the need for making a systematic expansion in powers of T/T_K and V/T_K .

The striking qualitative similarity between the two sets of curves in Fig. 4 can be made quantitative by using T_K as a fitting parameter: the choice of T_K determines which curves in Fig. 4(a) and (b) are to be associated with each other. Choosing $T_K = 8K$ for sample 1, HKH are able to get “quite good”¹³ simultaneous agreement between a significant number of the individual experimental data curves and their NCA curves of corresponding temperature. This is illustrated in Fig. 5³⁰ for 3 curves from sample # 1. In other words, *by using a single fitting parameter, T_K , HKH can obtain good quantitative agreement between the NCA and experimental conductance curves for a whole set of curves*.

B. Comparison of CFT and NCA Results with Experimental Scaling Curve

Let us denote the result of plotting a given NCA numerical $G(V, T)$ curve in the maximally normalized form of Eq. (61) by $\Gamma(v, T) - 1$. Fig. 4(a) shows that for sufficiently small T , the $\Gamma_T(v, T) - 1$ curves for different T all overlap, i.e. the NCA results show good scaling as $T \rightarrow 0$, in agreement with the CFT prediction. The $\Gamma(v, T)$ curve with the smallest T calculated by HKH, namely $T/T_K = 0.003$, is the most likely to agree with the CFT result for $\Gamma(v)$, since for this curve the T/T_K deviations from perfect scaling, which are neglected in the CFT calculation, are smallest.

In Fig. 6 we show the three experimental scaling curves of Fig. 11 of paper I (curves 1-3), the CFT prediction for $\Gamma(v) - 1$ from Eq. (56) (curve 4), and the NCA result for $\Gamma(v, T) - 1$, for $T/T_K = 0.003$ (curve 5) and $T/T_K = 0.08$ (curve 6). All these curves have been rescaled into the “maximally normalized form” of Eq. (57). We see that there is rather good agreement between the CFT curve and the $T/T_K = 0.003$ NCA result. The

experimental scaling curves agree with neither of these, but agree remarkably well with the $T/T_K = 0.08$ NCA curve.

To make these statements quantitative, we compare the values for the universal constant Γ_1 , defined as follows from the asymptotic large- v expansion of $\Gamma(v) - 1$ [compare Eq. (27) of paper I]:

$$\Gamma(v) - 1 \equiv v^{1/2} + \Gamma_1 + O(v^{-1/2}). \quad (62)$$

Γ_1 is the y -intercept of the asymptotic slope of the curve $\Gamma(v) - 1$ vs. $v^{1/2}$, extrapolated back to $v = 0$. It measures “how soon the scaling curve bends up” towards linear behavior, and is the single parameter that most strongly characterizes the scaling function (which is otherwise rather featureless). We find the following values for Γ_1 :

$$\begin{aligned} \Gamma_1^{CFT} &= -1.14 \pm 0.10, & \Gamma_1^{NCA}(T/T_K = 0.003) &= -1.12 \pm 0.10, \\ \Gamma_1^{EXP} &= -0.75 \pm 0.16, & \Gamma_1^{NCA}(T/T_K = 0.08) &= -0.74 \pm 0.10. \end{aligned} \quad (63)$$

Hence, the CFT and NCA calculations for $T/T_K = 0.003$ agree rather well, which inspires confidence in the general reliability of the NCA method at very low energies.

The agreement between the experimental curves and the $T/T_K = 0.08$ NCA curve could actually have been anticipated, for the following reason: HKH determined their (only) fitting parameter T_K by choosing the value (namely $T_K = 8$ K) that produces the best agreement between the few *lowest-T* curves in their set of calculated $G(V, T)$ curves and the corresponding experimental ones. Thus, the very lowest T -curve in the experiment (with $T = 0.6$ K) is well-reproduced by the corresponding NCA curve (with $T/T_K = 0.08$) because T_K was specifically chosen to produce this agreement.¹⁷

It is somewhat surprising, though, that the difference between the $T/T_K = 0.003$ and $T/T_K = 0.08$ NCA curves is so large. Perfect scaling would require all the various $\Gamma_T(v)$ curves for different T to overlap, and the fact that they do not shows that the deviations from perfect scaling which are expected to develop as T/T_K grows are already significant at values as small as $T/T_K = 0.08$.

Thus, as first pointed out by HKH, the NCA results imply that *the T/T_K corrections to the universal scaling curve that were neglected in the CFT calculation (see section V 3) are in fact not negligible in the present experiment*: T is still large enough that they matter, and the experimental scaling curve is *not* the truly universal one. This conclusion explains why the CFT and experimental scaling curves don’t agree; it also suggests that if the experiments were repeated at lower temperatures, better agreement might be achievable.

One might ask whether our conclusion that deviations from scaling are important are not in conflict with the claims in paper I [property (P6)] that the experimental curves show good scaling. The answer is that while the experimental curves do scale well, they do not scale quite well enough to reproduce “perfect” scaling. Perfect scaling requires that the curves overlap completely *when plotted in maximally normalized form* (as in figure 6), a procedure that involves rescaling the x -axis by a constant A to make the slope = 1. This procedure

¹⁷The NCA calculations achieved more, though, than merely fitting one curve with one parameter, because they succeeded in reproducing quite well a whole set of curves (see end of section VIA).

is clearly very sensitive: even curves that seem to collapse well onto the same scaling curve when not maximally normalized [as those in Fig. 4(b), or Fig. 8(b) of paper I], can show slight differences in slope in the regime of largish v when they begin to bend away from the ideal scaling curve (note that some uncertainty is involved in determining this slope, since the curves are not perfectly linear in this regime). When being brought into maximally normalized form, these curves will have their x -axes rescaled by different amounts to make all the slopes equal to 1 (the exact amount of rescaling needed being subject to the same uncertainty as the slope), and can by this rescaling be sufficiently deformed that they do not collapse onto each other any more. This is vividly illustrated by the observation that the $T/T_K = 0.003$ and 0.08 NCA curves, that in fact seem to overlap rather well in the non-maximally normalized form of figure 4(a), differ so markedly in the maximally normalized form of figure 6.

In short, maximal normalization is very efficient in revealing small deviations from perfect scaling, which is why the experimental data, which scales well when not maximally normalized, does not scale so well under maximal normalization.

One might be tempted to compare the CFT curve with experiment in non-maximally normalized form, where deviations from scaling do not reveal themselves so glaringly. However, this would not be meaningful, because the slope of the CFT scaling $\Gamma(v)$ curve is universal, whereas those of the experimental scaling curves are not (see figure 11(a) and the last paragraph of section V 2). The only meaningful comparison between CFT and experiment is in a form in which the non-universality of the experimental slopes has been rescaled away, i.e. the maximally normalized form.

From a theorist's point of view, the conclusion that the experimental scaling curve is not the universal one and that non-universal T/T_K corrections play a role is somewhat disappointing, since for a system about whose microscopic nature so little is known, the quantities that allow the most compelling comparison between theory and experiment are universal quantities, which are independent of the unknown details. However, disappointing or not, this is the message of Fig. 6.

Nevertheless, the good agreement between the CFT and NCA scaling curves, which confirms the reliability of the NCA method, combined with the good quantitative agreement between the NCA and the experimental conductance curves when T_K is used as fitting parameter, allows the main conclusion of this paper:

The 2-channel Kondo model is in quantitative agreement with the experimental scaling $G(V, T)$ data.

VII. SUMMARY AND CONCLUSIONS

The calculation of this paper was inspired by experiments of Ralph and Buhrman on ZBAs in quenched Cu nanoconstrictions (reviewed in paper I), which are qualitatively in accord with the assumption that the anomalies are caused by two-level systems in the constriction that interact with electrons according to Zawadowski's non-magnetic Kondo model, which is believed to renormalize, at sufficiently low temperatures, to the 2CK model.

To obtain a quantitative test of this interpretation of the experiment, we performed a calculation of the non-linear conductance $G(V, T)$ of a nanoconstriction containing 2-channel Kondo impurities, in the weakly non-equilibrium regime (weakly non-equilibrium regime)

of $V, T \ll T_K$, and extracted from it a certain universal scaling function $\Gamma(v)$, which we compare with experimental scaling function.

To model the experimental situation, we introduced a generalization of the bulk 2CK model, namely the naconstriction 2-channel Kondo model (NTKM), which keeps track of which lead (left or right) an electron comes from and is scattered into.

The main conceptual challenge in the calculation of $G(V, T)$ was how to deal with the non-equilibrium aspects of the problem. On the one hand, standard perturbative Keldysh approaches do not work for $T \ll T_K$, where perturbation theory breaks down for the Kondo problem. On the other hand, Affleck and Ludwig's conformal field theory solution (CFT) of the 2CK problem was worked out only for an equilibrium electron system.

Therefore we proposed a conceptually new strategy (outlined in section III, the heart of this paper) which combines ideas from CFT with the Hershfield's Y -operator formalulation of non-equilibrium problems: Hershfield showed that the calculation of non-equilibrium expectation values becomes simple when they are expressed in terms of the scattering states of the problem. We expressed these in terms of certain scattering amplitudes $\tilde{U}_{\eta\eta'}$, which we extracted from an equilibrium two-point function $G_{\eta\eta'} = -\langle T\psi_\eta\psi_{\eta'}^\dagger \rangle$ that is exactly known from CFT. (This procedure only gives their $V = 0$ values, but we proposed that in the non-Fermi-liquid regime the corrections of order V/T_K are negligible.) Once the $\tilde{U}_{\eta\eta'}$ were known, the calculation of the current was straightforward.

In the present paper, we implemented all parts of this strategy, except that which requires a detailed knowledge of CFT, namely the calculation of $G_{\eta\eta'}$. This is discussed in detail in paper III.

Our result for the scaling curve $\Gamma(v)$ does not agree with the experimentally measured scaling function, because terms of order T/T_K that are neglected in our calculation are apparently not sufficiently small in the experiment; however, when our results are combined with the numerical results of Hettler, Kroha and Hershfield¹³ (which implicitly do include the neglected terms), quantitative agreement of the 2CK calculations with the experimental results is achieved (see section VI B).

Thus we are able to conclude that the NTKM is in quantitative agreement with the experimental scaling data. This lends further support to the 2CK interpretation of RB's experiments, and the associated conclusion that they have indeed observed non-Fermi-liquid behavior.

However, the theoretical justification for assuming that the non-magnetic Kondo model will under renormalization flow into sufficiently close proximity of the non-Fermi-liquid fixed point of the 2CK model has recently been called into question. There are unresolved theoretical concerns^{12,15}, summarized in Appendix D, whether a realistic TLS-electron system will ever flow sufficiently close to this fixed point to exhibit the associated non-Fermi-liquid behavior, because of the inevitable presence of various relevant perturbations that can prevent the flow towards this fixed point.

Therefore, not all questions regarding the Ralph-Buhrman experiments have been resolved to everyone's satisfaction. In our opinion, the outstanding question that remains is: why does the 2CK interpretation of this experiment seem to work so well despite the concerns about the theoretical justification for assuming proximity to the 2CK model's non-Fermi-liquid fixed point? In view of the fact that at present no alternative explanation for the experiment is known that is in agreement with all experimental facts, we believe that

the question of the flow towards and stability of the non-Fermi-liquid fixed point of the non-magnetic Kondo problem is worthy of further theoretical investigation.

Acknowledgements: It is a pleasure to thank D. Ralph and R. Buhrman for an extremely stimulating collaboration, and D. L. Cox, D. Fisher, S. Herschield, M. Hettler, Y. Konddev, J. Kroha, M. Moustakas, A. Schiller, N. Wingreen, G. Zaránd and in particular A. Zawadowski for discussions. This work was partially supported by the MRL Program of the National Science Foundation, Award No. DMR-9121654, and Award No. DMR-9407245 of the National Science Foundation.

APPENDIX A: SEMICLASSICAL DESCRIPTION OF NON-EQUILIBRIUM TRANSPORT

In order to motivate the form of the free density matrix ρ_o introduced in section II B, we recall in this appendix some standard results from the semi-classical theory of non-equilibrium transport through a ballistic nanoconstriction. Usually, this is described using a semi-classical Boltzmann formalism to calculate the semi-classical electron distribution function $f_{\vec{k}}(\vec{r})$ and the electrostatic potential energy $e\phi(\vec{r})$. This was first worked out in^{32,33}; a very careful treatment may be found in³⁴, which is well-reviewed in²⁰. A more up-to-date review is³⁵.

In the semi-classical strategy, one first calculates $f_{\vec{k}}^{(0)}(\vec{r})$ and $e\phi^{(0)}(\vec{r})$, the distribution function and electrostatic potential in the absence of any electron scattering mechanism, and thereupon uses these functions to calculate the backscattering current due to electrons that are backscattered while attempting to traverse the hole. The results for $f_{\vec{k}}^{(0)}(\vec{r})$ and $e\phi^{(0)}(\vec{r})$ are standard and shown in Figs. 2 and 3.¹⁸ Fig. 2 is a position-momentum space hybrid, showing $f_{\vec{k}}^{(0)}(\vec{r})$ at $T = 0$, with its \vec{k} -space origin drawn at the position \vec{r} to which it corresponds. One can understand Fig. 2(a) almost without calculation, simply by realizing that in the absence of collisions, electrons will maintain a constant total energy $E_{\vec{k}}$. Thus, an electron that is injected from $z = \pm\infty$ in the R/L lead with total energy $E_{\vec{k}}(z = \pm\infty) = \varepsilon_{\vec{k}} \pm eV/2$ and traverses the hole, will experience a change in its potential energy from $e\phi(\pm\infty) = \pm eV/2$ to $e\phi(\mp\infty) = \mp eV/2$ and hence accelerate or decelerate in such a way that $E_{\vec{k}}(\vec{r}) = \varepsilon_{\vec{k}} + e\phi(\vec{r})$ remains constant.

The key feature of Fig. 2 is that the distribution of occupied electron states in momentum space, at any point \vec{r} in the vicinity of a ballistic constriction, is highly anisotropic and consists of *two* sectors, to be denoted by L and R . The L/R sector contains the momenta of all electrons that are *incident as L/R -movers*, i.e. originate from the $\pm V/2$ or R/L side of the device, *and* have reached \vec{r} along ballistic straight-line paths, including paths that traverse the hole (the bending of paths due to the electric field is of order eV/ε_F and hence negligible). At a given point \vec{r} , the momentum states in the L/R sectors are filled up to a maximum energy of $(E_{\vec{k}}(\vec{r}))_F$ which, because of energy conservation along trajectories, is

¹⁸Our figures and arguments are given for the case $eV > 0$. We take $e = -|e|$ and hence $V = -|V|$. With $\mu \pm eV/2$ for R/L leads, there then is a net flow of electrons from right to left, and the current to the right is positive.

equal to $\mu \pm eV/2$, the Fermi energy at $z = \pm\infty$ from where the electrons were injected. Thus, for \vec{k} in the L/R sector, one finds

$$f_{\vec{k} \in L/R}^{(0)}(\vec{r}) = f_o \left[E_{\vec{k}}(\vec{r}) - \left(E_{\vec{k}}(\vec{r}) \right)_f \right] = f_o \left[\varepsilon_{\vec{k}} - \left(\mu \pm eV/2 - e\phi^{(0)}(\vec{r}) \right) \right]. \quad (\text{A1})$$

Fig. 3 shows that $e\phi^{(0)}(\vec{r})$ changes smoothly from $-eV/2$ to $+eV/2$ (the change occurs within a few constriction radii a from the hole). It is worth emphasizing, though, that the electrostatic potential energy $e\phi(\vec{r})$ plays only an indirect role when it comes to calculating low-energy (i.e. $T/\varepsilon_F, V/\varepsilon_F \ll 1$) transport properties. The reason is simply that the only role of $e\phi(\vec{r})$ is to define the *bottom* of the conduction band, hence causing acceleration and deceleration of electrons to maintain $E_{\vec{k}}(\vec{r}) = \text{constant}$. Low-energy transport properties, however, are determined by what happens at the *top* of the conduction band, in particular by the sharply anisotropic features characterizing Fig. 2 and Eq. (A1).¹⁹

The above considerations suggest that the essence of the non-equilibrium nature of the problem will be captured correctly if we adopt the following simplified picture: ignore the spatial variation of the electrostatic potential $e\phi(\vec{r})$ altogether, and simply consider two leads (R/L) with chemical potentials (measured relative to the equilibrium μ) $\mu_\eta = \sigma \frac{1}{2} eV$, which inject L/R -moving ballistic electrons into each other (recall that $\sigma = (+, -)$ for (L, R) -movers). The two leads are assumed infinitely large and hence “independent and unperturbed”, in the sense that their thermal distribution properties are not perturbed when a small number of electrons are transferred from one to the other. This simplified picture is the basis for the Ansatz (4) for the free density matrix ρ_o in section II B.

APPENDIX B: THE BULK NON-MAGNETIC KONDO MODEL

In this appendix we recall some basic properties of Zawadowksi’s non-magnetic (or orbital) Kondo model for the interaction of a TLS with conduction electrons in a bulk metal. Thus, this appendix provides the background material that was assumed known when we introduced the introduction of the nanoconstriction two-channel Kondo model in section II. Zawadowski proposed his model in Ref.⁸, subsequently developed it with his coworkers in Refs.^{36,9,37,38,39}, and rather recently, together with Zaránd, introduced some important refinements^{40,41,42,43}. Brief, lengthy and exhaustive reviews may be found in^{16,44} and⁴⁵, respectively.

¹⁹This is illustrated, for example, in the calculation of the Sharvin formula for the conductance G_o of the a circular constriction (radius a) in the absence of scattering²⁰:

$$I_o = \int_{\text{hole}} dx dy \frac{2e}{\text{Vol}} \sum_{\vec{p}} (v_{\vec{p}})_z f_{\vec{p}}(x, y, z = 0) = a^2 e^2 m \varepsilon_F / (2\pi \hbar^3 |V|). \quad (\text{A2})$$

It depends on the electrostatic potential only through $e\phi(x, y, z = 0) = 0$, and it is easy to verify that the V -dependence arises solely from the L/R anisotropy of $f_{\vec{p}}(x, y, z = 0)$.

1. Zawadowski's Bulk Bare Model

Consider a tunneling center (TC) in a bulk smetal, i.e. an atom or group of atoms that can hop between two different positions inside the metal, modelled by a double-well potential [see Fig. 1, and Fig. 6 of I]. At low enough temperatures and if the barrier is sufficiently high, hopping over the barrier through thermal activation becomes negligible. However, if the separation between the wells is sufficiently small, the atom can still move between them by tunneling.

If the tunneling is *slow* (hopping rates⁴⁵ $\tau^{-1} < 10^8 s^{-1}$), the atom is coupled only to the density fluctuations of the electron sea, which can be described by a bosonic heat bath^{46,47}. The tunneling is then mainly incoherent, and the only effect of the electron bath is to “screen” the tunneling center: an electron screening cloud builds up around the center and moves adiabatically with it, which leads to a reduced tunneling rate due to the non-perfect overlap of the two screening clouds corresponding to the two positions of the tunneling center.

In this paper we are interested only in the case where the tunneling is *fast* (at rates⁴⁵ $10^8 s^{-1} < \tau^{-1} < 10^{12} s^{-1}$), in which case the tunneling center is usually called a two-level system (TLS) [though in this appendix and the next we shall continue to call it a tunneling center, because in general more than two states can be associated with it, see Eq. (B2)]. Then the energy corresponding to the tunneling rate, determined by the uncertainty principle, is in the range 1 mK to 10 K. (If the tunneling is “ultra-fast” ($\tau^{-1} > 10^{12} s^{-1}$), the energy splitting $E_2 - E_1$ between the lowest two eigenstates due to tunneling becomes too large ($> 10K$) and the interesting dynamics is frozen out.) Moreover, the TLS-electron coupling is assumed strong enough that in addition to screening, an electron scattering off the tunneling center can *directly induce* transitions between the wells: it can either induce direct tunneling through the barrier (*electron-assisted tunneling*), or excite the atom to an excited state in one well, from where it can decay across to the other well (*electron-assisted hopping* over the barrier).

To describe such a system, Zawadowski introduced the following model. The Hamiltonian is the sum of three terms:

$$H = H_{TC} + H_{el} + H_{int} . \quad (B1)$$

The first term describes the motion of the tunneling center the double well, in the absence of electrons [see Fig. 1, and Fig. 6 of I]:

$$H_{TC} = \sum_a E_a b_a^\dagger b_a . \quad (B2)$$

This problem is considered to be already solved: the energies E_a ($E_1 < E_2 < \dots$) are the exact eigenenergies of the exact eigenstates $|\Psi_a\rangle = b_a^\dagger |0\rangle$ of the tunneling center, with corresponding wave-functions $\varphi_a(\vec{R})$. The spectrum will contain two nearly-degenerate energies E_1 and E_2 , split by an amount $E_2 - E_1$, corresponding to even and odd linear combinations of the lowest-lying eigenstates of each separate well; the remaining energies, collectively denoted by E_{ex} , correspond to more highly excited states in the well, with $E_{ex} - E_2$ typically on the order of the Debye temperature of the metal, i.e. several hundred Kelvin.

The tunneling center-electron interaction is described by a pseudo-potential $V(\vec{R} - \vec{r})$, which describes the change in energy of the tunneling center at position \vec{R} due to the presence of an electron at position \vec{r} , and is assumed to depend only on the relative coordinate $\vec{r} - \vec{R}$:

$$H_{int} = \sum_i \int d^3\vec{r} \Psi_i^\dagger(\vec{r}) \Psi_i(\vec{r}) V(\vec{r} - \vec{R}) \int d\vec{R} \sum_{aa'} b_a^\dagger \varphi_a^*(\vec{R}) b_{a'} \varphi_{a'}(\vec{R}) , \quad (B3)$$

where $\Psi_i(\vec{x}) = (\text{Vol})^{-1/2} \sum_{\vec{p}} e^{i\vec{p}\cdot\vec{x}} c_{o\vec{p}i}$. Here $c_{o\vec{p}i}^\dagger$ creates a *free* electron (hence the subscript o) with momentum \vec{p} ($= p\hat{p}$), energy ε_p (assumed independent of the direction \hat{p} or $\Omega_{\hat{p}}$ of \vec{p}) and Pauli spin $i = \uparrow, \downarrow$ (we use the index i because this will turn out to be the channel index). Terms in Eq. (B3) with $a \neq a'$ correspond to transitions between eigenstates of the tunneling center induced by the scattering of an electron.

Now, let $\{F_\alpha(\hat{p})\}$ be any complete set of orthogonal functions of \hat{p} (e.g. $F_\alpha(\hat{p}) = \sqrt{4\pi} Y_{lm}(\hat{p})$, but in principle any set of orthogonal angular functions can be used), labelled by a discrete index α and satisfying

$$\sum_\alpha F_\alpha^*(\hat{p}) F_\alpha(\hat{p}') = 4\pi \delta(\hat{p} - \hat{p}') , \quad \int \frac{d\Omega_{\hat{p}}}{4\pi} F_\alpha^*(\hat{p}) F_{\alpha'}(\hat{p}) = \delta_{\alpha\alpha'} . \quad (B4)$$

Then the electrons' continuous direction index \hat{p} can be traded for the discrete index α by making a unitary transformation (N_o is the density of states per spin at ε_F):

$$c_{o\varepsilon\alpha i} = N_o^{1/2} \int \frac{d\Omega_{\hat{p}}}{4\pi} F_\alpha^*(\hat{p}) c_{o\vec{p}i} , \quad c_{o\vec{p}i} = N_o^{-1/2} \sum_\alpha F_\alpha(\hat{p}) c_{o\varepsilon\alpha i} , \quad (B5)$$

The new set of operators $\{c_{o\varepsilon\alpha i}\}$ are labelled by the continuous energy index ε ($= \varepsilon_p$) and the discrete index α , to be called the conduction electron *pseudo-spin index*, for reasons that will become clear below.

In the new basis, the electrons kinetic energy and interaction with the tunneling center can be written in the following form:

$$H_o = \int_{-D}^D d\varepsilon \sum_\alpha \varepsilon c_{o\varepsilon\alpha i}^\dagger c_{o\varepsilon\alpha i} , \quad (B6)$$

$$H_{int} = \sum_{\alpha\alpha'} \sum_{aa'} \int_{-D}^D d\varepsilon \int_{-D}^D d\varepsilon' v_{\alpha\alpha'}^{aa'} c_{o\varepsilon\alpha i}^\dagger c_{o\varepsilon'\alpha' i} b_a^\dagger b_{a'} . \quad (B7)$$

For simplicity, the standard assumptions were made that electron energies lie within a band of width $2D$, symmetric about ε_F , with constant density of states N_o per α, i species, and that the energy dependence of the coupling constants $v_{\alpha\alpha'}^{aa'}$ can be neglected. (These assumptions are justified by the fact that the Kondo physics to be studied below is dominated by excitations close to the Fermi surface.) The $v_{\alpha\alpha'}^{aa'}$ are volume-independent, dimensionless constants (typically of order 0.1 or smaller), whose exact values are determined by the potential $V(\vec{r} - \vec{R})$ and the tunneling center eigenstates $\varphi_a(\vec{R})$.

Written in this form, the interaction has the form of a generalized, anisotropic Kondo interaction: a and α can be regarded as impurity- and electron *pseudo-spin* indices (since α takes on infinitely many values, the electrons have an infinitely large pseudo-spin), and the interaction describes electron-induced “spin-flip” transitions of the impurity. Note, however,

that because the nature of the interaction is non-magnetic (to which fact the model owes its name), the interaction is diagonal in the Pauli spin index $i = (\uparrow, \downarrow)$. Thus we have two identical *channels* of conduction electrons, the $\{c_{o\varepsilon\alpha\uparrow}^\dagger\}$ - and the $\{c_{o\varepsilon\alpha\downarrow}^\dagger\}$ operators, and accordingly i is called the *channel* index.

2. The Renormalized Bulk Model

The formal similarity of the interaction of Eq. (B7) with the Kondo interaction implies that here too perturbation theory will fail at temperatures below a characteristic Kondo temperature T_K , leading to complicated many-body physics as $T \rightarrow 0$ and a strongly correlated ground state. Perturbation theory fails for $T < T_K$ because the effective (T -dependent) coupling constants $v_{\alpha\alpha'}^{aa'}$ grow as T decreases, and eventually become too large (see Fig. 8 in Appendix C). The way in which this happens was studied in great detail by Zawadowski and co-workers. Using Anderson's poor man's scaling technique to analyse the renormalization group evolution of the bare model, they concluded that the renormalized model to which it flows as the temperature is lowered is⁴⁸ the *isotropic two-channel Kondo model* (see Eq. (B10) below). Below we briefly give the starting point and final result of their poor man's scaling analysis. A summary of the intermediate steps and main assumptions made along the way can be found in Appendix C.

The interaction vertex, calculated to second order in perturbation theory, is given by the following expression:

$$\Gamma_{\varepsilon\alpha\varepsilon'\alpha'}^{aa'} = v_{\alpha\alpha'}^{aa'} + \sum_{b\beta} \int_{-D}^D d\bar{\varepsilon} \times \left[v_{\alpha\beta}^{ab} v_{\beta\alpha'}^{ba'} \frac{1 - f_\beta(\bar{\varepsilon})}{\varepsilon' + E_{a'} - (\bar{\varepsilon} + E_b)} - v_{\beta\alpha'}^{ab} v_{\alpha\beta}^{ba'} \frac{f_\beta(\bar{\varepsilon})}{\varepsilon' + E_{a'} - (-\bar{\varepsilon} + \varepsilon' + \varepsilon + E_b)} \right] \quad (B8)$$

$$\simeq v_{\alpha\alpha'}^{aa'} + \sum_{b\beta} \ln [\max\{E_{a'}, E_b, T, \varepsilon, \varepsilon'\}/D] \left[v_{\alpha\beta}^{ab} v_{\beta\alpha'}^{ba'} - v_{\alpha\beta}^{ba'} v_{\beta\alpha'}^{ab} \right], \quad (B9)$$

To obtain the second line, only the logarithmic terms were retained.

Note the occurrence of the "commutator" $\left[v_{\alpha\beta}^{ab} v_{\beta\alpha'}^{ba'} - v_{\alpha\beta}^{ba'} v_{\beta\alpha'}^{ab} \right]$; the fact that this is in general non-zero, due to the non-trivial angular dependence of the coupling constants, is crucial for the presence of logarithmic corrections (and is the reason why this model is sometimes called a *non-commutative* model).

Now Anderson's poor man's scaling RG⁴⁹ is implemented: one changes the bandwidth from D to a slightly smaller D' , and compensates this change by introducing new coupling constants that depend on $x = \ln D/D'$, namely $v = v(x)$, with the x -dependence chosen such that $\Gamma_{\alpha\alpha'}^{aa'}$ remains invariant. The procedure is repeated successively until D' reaches $E_{max} = \max\{E_{a'}, E_b, T, \varepsilon, \varepsilon'\}$, at which point the RG flow is cut off, and the resulting renormalized model, with coupling constants $v(\ln(D/E_{max}))$, has to be analyzed anew.

The upshot of a lengthy analysis (summarized in Appendix C) is the following: All but the lowest two of the excited states of the tunneling center decouple from the interaction,

which eventually involves an impurity with effectively only two states,²⁰ $a = 1, 2$ (i.e. a TLS with an effective pseudo-spin $S_{imp} = 1/2$), with a renormalized splitting $E_2 - E_1 \equiv \Delta$ and Hamiltonian $H_{tunnelingcenter} = \sum_{a,a'=1,2} b_a^\dagger (\frac{1}{2} \Delta \sigma_{a,a'}^z) b_{a'}$. Likewise, for the conduction electrons all but two of the pseudo-spin degrees of freedom, which we label by $\alpha = 1, 2$, decouple from the interaction. These two “surviving” channels, $c_{o\epsilon 1i}^\dagger$ and $c_{o\epsilon 2i}^\dagger$, are in general two complicated linear combinations of the initial $c_{o\epsilon \alpha i}^\dagger$ ’s. They represent those two angular degrees of freedom that initially were coupled most strongly to the impurity and for which the couplings hence grow faster under the renormalization group than those of all other channels (which hence effectively decouple). Furthermore, the resulting effective interaction is spin-isotropic (spin-anisotropy can be shown to be an irrelevant perturbation²⁶), so that the effective interaction can be written in the form [see Eq. (C15)]:

$$H_{int} = \int d\epsilon \int d\epsilon' \sum_{\alpha\alpha'=1,2} \sum_{aa'=1,2} \sum_{i=\uparrow,\downarrow} v_K \left(c_{o\epsilon \alpha i}^\dagger \frac{1}{2} \vec{\sigma}_{\alpha\alpha'} c_{o\epsilon' \alpha' i} \right) \cdot \left(b_{a'}^\dagger \frac{1}{2} \vec{\sigma}_{aa'} b_{a'} \right) . \quad (B10)$$

Here v_K is the magnitude of the effective tunneling center-electron coupling (and estimated^{42, Table 1} to be of order $v_K \simeq 0.1 - 0.2$). Thus, *the effective Hamiltonian²¹ has exactly the form of the isotropic, magnetic 2CK problem, with impurity pseudo-spin $S_{imp} = 1/2$ ($a = 1, 2$), electron pseudo-spin $s_{el} = 1/2$ ($\alpha = 1, 2$), and the Pauli spin $i = \uparrow, \downarrow$ as channel index.*

When the temperature is lowered even further, then, provided that $\Delta = 0$, this model flows towards a non-trivial, *non-Fermi-liquid fixed point* at $T = 0$, at which the system shows non-Fermi-liquid behavior^{10,11}. However, Δ is a relevant perturbation (with scaling dimension $-\frac{1}{2}$, see section VII C of I). This means that if $\Delta \neq 0$, the flow towards the non-Fermi-liquid fixed point will be cut off when T becomes smaller than Δ^2/T_K , after which the flow will be towards a different, Fermi-liquid fixed point that corresponds to potential scattering off a static impurity. In subsequent sections we shall always adopt assumption (A2) of paper I (for reasons explained in section VII C of paper I) namely that Δ is sufficiently small relative to T ($\Delta \ll \sqrt{T T_K}$) that the physics *is* governed by the non-Fermi-liquid fixed point, and that the departure of the flow from the latter towards the Fermi-liquid fixed point has not yet started.

It is tempting to propose for the effective Hamiltonian of Eq. (B10) the following physical interpretation (which is given in this form by Moustakas and Fisher¹⁵, and can be viewed as complimentary to Zawadowski’s picture of electron-induced tunneling). A charged impurity in a metal will be screened by a screening cloud of electrons, which can be thought of as part of the “dressed” impurity. If the impurity is a two-state system, it will drag along its tightly bound screening cloud as it tunnels between the wells. In doing so, it will redistribute

²⁰The two states are considered here in the energy representation, i.e. their wavefunctions are $\varphi_{1,2} = \frac{1}{\sqrt{2}}(\varphi_r \pm \varphi_l)$ in terms of the wavefunctions φ_r or φ_l describing the tunneling center localized mainly in the r or l wells.

²¹Of course, the flow toward the isotropic 2CK model only happens provided that all relevant perturbations that would drive the system away from this fixed point are sufficiently small – this implicit assumption will be critically discussed in Appendix D.

the low-energy excitations near the Fermi surface. In particular, it will likely interact most strongly with two spherical waves of low-energy electrons, “centered” on the two impurity positions in the left and right wells^{9,p.1575}, with which one can associate a pseudo-spin index $\alpha = L, R$. Now, when the impurity and its screening cloud tunnels from the left to the right well, low-energy electrons around the right well will move in the opposite direction to the left well, to compensate the movement of electronic charge bound up in the screening cloud, and thereby to decrease the orthogonality between the pre- and post-hop configurations. Thus, a flip in the impurity pseudo-spin is always accompanied by a flip in electron pseudo-spin, as in Eq. (B10). In two very recent papers¹⁵, Moustakas and Fisher have used this interpretation as a starting point for a related but not quite equivalent description of the tunneling center-electron system¹⁵.

APPENDIX C: POOR MAN’S SCALING ANALYSIS OF BULK NON-MAGNETIC KONDO MODEL

In this appendix, we summarize, following the recent papers by Zaránd and Zawadowski^{41,42} and Zaránd^{43,50}, the poor man’s scaling arguments that suggest that the bare, equilibrium non-magnetic Kondo model of Eq. (B3) renormalizes to the isotropic 2-channel Kondo model Eq. (B10). It should be mentioned at the outset, though, that the ensuing analysis has a somewhat heuristic character, since it employs scaling equations derived in the weak-coupling limit, based on perturbation theory in the coupling constants. Since such scaling equations cease to be strictly valid as soon as one scales into strong-coupling regions of parameter space, by such an analysis the conclusion that the bare model flows towards the 2CK model can at best be made plausible, and never be proven conclusively. In fact, this conclusion has recently been called into question^{12,15}, on the basis of theoretical considerations (controversial themselves¹⁷), that are discussed in Appendix D.

1. Hamiltonian and Initial Parameters

The starting point is the Hamiltonian introduced and motivated in Appendix B, written in the form of Eqs. (B2), (B6) and (B7). Let $\Delta_b = E_2 - E_1$ be the bare energy difference between the two lowest-lying eigenstates, nearly degenerate eigenstates of the well. The remaining energies, E_a , $a = 3, 4, \dots$, collectively denoted by E_{ex} , correspond to more highly excited states in the well.

We are interested in the regime where $\Delta_b \ll T \ll E_{ex} \ll D$. Hence we take $\Delta_b \simeq 0$, i.e. consider a symmetrical double well with a two-fold degenerate ground state. It is then convenient to make a change of basis from the exact symmetrical and anti-symmetrical ground states $|\Psi_1\rangle$ and $|\Psi_2\rangle$ to the right and left states $|r\rangle$ and $|l\rangle = \frac{1}{\sqrt{2}}(|\Psi_1\rangle \pm |\Psi_2\rangle)$.

Note that, since a non-zero bare tunneling matrix element (Δ_0) between the wells always leads to a splitting $E_1 - E_2 \simeq \Delta_o$, by taking $\Delta_b \simeq 0$ we are also implicitly assuming that $\Delta_o \ll T$. This means that direct tunneling events are very unlikely, raising the question of

whether Kondo-physics will occur at all.²² However, the inclusion of excited states in the model overcomes this potential problem as follows^{41,42}: a careful estimate of the coupling constants⁴⁰ in terms of the overlap integrals (B3) has shown that

$$|v^{r,l}| \simeq 10^{-3} |v^{l,l} - v^{r,r}|, \quad |v^{l,ex}| \simeq |v^{r,ex}| \simeq |v^{l,l} - v^{r,r}|. \quad (C1)$$

The first relation reflects the fact that direct electron-assisted tunneling, parameterized by $|v^{r,l}|$, is proportional to the bare tunneling rate Δ_o and hence very small. However, the second relation shows that the matrix elements for electron-assisted transitions to excited states, parametrized by $|v^{l,ex}|$ and $|v^{r,ex}|$, are of the same order of magnitude as for the usual ‘‘screening term’’ $|v^{l,l} - v^{r,r}|$ [this is because the overlap integrals in Eq. (B3) are larger for $\varphi_{ex}^* \varphi_{r,(l)}$ than for $\varphi_r^* \varphi_l$, since the excited state wave-function spreads over both wells (see Fig. 1)]. Although the amplitudes for such processes are proportional to the factor $1/E_{ex}$ (which is small, since E_{ex} is large), Zarnd and Zawadowski showed that such terms also grow under scaling [see Eq. (C3) below], and eventually lead to a renormalized model which has sufficiently large effective tunneling amplitudes to display Kondo physics.

2. Poor Man’s Scaling RG

The interaction vertex, calculated to second order in perturbation theory from the diagrams in Fig. 7(a), is given by Eq. (B9):

$$\Gamma_{\varepsilon\alpha\varepsilon'\alpha'}^{aa'} = v_{\alpha\alpha'}^{aa'} + \sum_{b\beta} \ln [\max\{E_{a'}, E_b, T, \varepsilon, \varepsilon'\}/D] \left[v_{\alpha\beta}^{ab} v_{\beta\alpha'}^{ba'} - v_{\alpha\beta}^{ba'} v_{\beta\alpha'}^{ab} \right]. \quad (C2)$$

Now Anderson’s poor man’s scaling RG⁴⁹ is implemented (very nicely explained in^{45,sections 3.2.2}): electron or hole excitations with large energy values do not directly participate in *real* physical processes; their only effect occurs through virtual excitations of the low-energy states to intermediate high-energy states. Hence such processes may be taken into account by introducing renormalized coupling parameters, which sum up all the virtual processes between a new, slightly smaller cut-off D' and the original D . In other words, all virtual processes between the energies D' and D are integrated out and their contributions are incorporated in new, D' -dependent coupling constants. This procedure is repeated for smaller and smaller D' , until D' becomes on the order of $\max\{E_c, T, \varepsilon_{p'}\}$.

Concretely, this is done by writing $v_{\alpha\alpha'}^{a,b} = v_{\alpha\alpha'}^{a,b}(x)$, where $x = \ln(D'/D)$ and the x -dependence of the coupling constants is determined by the requirement that the interaction vertex be invariant under poor man’s scaling, i.e. $\partial_x \Gamma_{\alpha\alpha'}^{a,b} = 0$. By Eq. (C2), this leads to the following *leading-order scaling equation*:

²²This was a serious limitation of Zawadowski’s original model, which did not include excited states: to give non-trivial many-body physics (i.e. a sufficiently large Kondo energy T_K), the bare tunneling rate Δ_o could not be too small; yet at the same time, the model only flows to the interesting non-Fermi liquid fixed point if $E_1 - E_2 \ll T$. This would have required a rather delicate and perhaps questionable fine-tuning of parameters. This problem has been overcome by including excited states in the model^{41,42}, as explained above.

$$\partial_x \underline{v}^{a,b}(x) = \sum_c \theta(D' - E_c) [\underline{v}^{a,c}(x), \underline{v}^{c,b}(x)] , \quad (C3)$$

where we have adopted the matrix notation $v_{\alpha\alpha'}^{a,b} \equiv \underline{v}^{a,b}$. [The significance of $\theta(D' - E_c)$ is explained in section C 5.] This equation, to be solved with the boundary condition $\underline{v}^{a,b}(0) = (\underline{v}^{a,b})_{bare}$, determines the nature of the RG flow away from the weak-coupling limit.

In the following two sections we outline the results obtained by Zawadowski and co-workers concerning the nature of the fixed point that the Hamiltonian flows towards as it scales out of the weak-coupling region. However, the arguments that are to follow all have a somewhat heuristic character: since they are based on scaling equations that were derived in the weak-coupling limit, based on perturbation theory in the coupling constants, in principle they cease to be strictly valid as soon as one scales into strong-coupling regions of parameter space. (The only method that gives quantitatively reliable results for the cross-over region is Wilson's numerical NRG^{51,52,53,26,54}.) Many of the results obtained below are therefore of mainly qualitative value, and not expected to be quantitatively accurate.

3. Scaling to 2-D Subspace

Let us for the moment consider the model without any excited tunneling center states, i.e. with $\sum_c = \sum_{r,l}$ (as was done in the first papers^{8,36,9}), postponing the more general case to section C 5. In this case, the coupling constants $\underline{v}^{a,b}(x)$ can be expanded in terms of Pauli matrices in the 2-dimensional space of the tunneling center (in the $l-r$ basis),

$$v_{\alpha\alpha'}^{a,b}(x) = \sum_{A=0}^3 \tilde{v}_{\alpha\alpha'}^A(x) \sigma_{a,b}^A , \quad a, b = l, r , \quad (C4)$$

where $A = (0, 1, 2, 3) = (0, x, y, z)$ and $\sigma_{ab}^0 \equiv \delta_{ab}$. The v^z term is called the *screening* term, and characterizes the difference in scattering amplitudes for processes in which an electron scatters from the atom in the right or left well *without* inducing a transition to the other well. The v^x and v^y terms are called *electron-assisted tunneling* terms, and describe the amplitude for processes in which the scattering of an electron induces the tunneling center to make a transition to the other well. According to Eq. (C1), $\tilde{v}^x \simeq \tilde{v}^y \ll \tilde{v}^z$. If one chooses the wave-functions of the tunneling center to be real, time-reversal invariance requires $\tilde{v}^y = 0$ (see^{9,(a),eq.(2.11)}).

The problem is now formally analogous to a (very anisotropic) magnetic Kondo problem in which a spin- $\frac{1}{2}$ impurity is coupled to conduction electrons with very large pseudo-spin (since α takes on a large number of values). However, Vladár and Zawadowski (VZ) have shown^{9,(a),section III.C} that (with realistic choices of the initial parameters) the problem always scales to a 2-dimensional subspace in the electron's α -index, so that the electrons have pseudo-spin $S_e = \frac{1}{2}$ (this happens independent of the signs of the initial couplings, see section C 4). Their argument goes as follows:

In the notation of Eq. (C4), the scaling equation (C3) takes the form^{9,p.1573,eq.(3.3)}

$$\frac{\partial \underline{v}^A}{\partial x} = -2i \sum_{BC} \varepsilon^{ABC} \underline{v}^B \underline{v}^C . \quad (C5)$$

Since $\tilde{v}^x \ll \tilde{v}^z$ and $\tilde{v}^y = 0$, Eq. (C5) can be linearized in \underline{v}^x and \underline{v}^y . VZ solved the linearized equations in a basis in α -space in which $\tilde{v}_{\alpha\beta}^z(0)$ is diagonal [$\tilde{v}_{\alpha\beta}^z(0) = \delta_{\alpha\beta}\tilde{v}_\alpha^z(0)$], and obtained the following solution^{9,p.1576,eq.3.17}:

$$\tilde{v}_{\alpha\beta}^z(x) = \delta_{\alpha\beta}\tilde{v}_\alpha^z(0) \quad (C6)$$

$$\tilde{v}_{\alpha\beta}^x(x) = \tilde{v}_{\alpha\beta}^x(0) \cosh 2x \left[\tilde{v}_\beta^z(0) - \tilde{v}_\alpha^z(0) \right], \quad (C7)$$

$$\tilde{v}_{\alpha\beta}^y(x) = i\tilde{v}_{\alpha\beta}^x(0) \sinh 2x \left[\tilde{v}_\beta^z(0) - \tilde{v}_\alpha^z(0) \right]. \quad (C8)$$

Barring unforeseen degeneracies in the matrix \tilde{v}^z , this shows that the two elements of \tilde{v}^z which produce the largest difference $|\tilde{v}_\beta^z(0) - \tilde{v}_\alpha^z(0)|$ will generate the most rapid growth in the corresponding couplings $\tilde{v}_{\alpha\beta}^x(x)$ and $\tilde{v}_{\alpha\beta}^y(x)$. In fact, since this growth is exponentially fast, any couplings with only slightly smaller $|\tilde{v}_\beta^z(0) - \tilde{v}_\alpha^z(0)|$ will grow much slower and hence decouple. Thus, we conclude that according to the leading-order scaling equations, the system *always renormalizes to a 2-D subspace in which the electrons have pseudo-spin $S_e = \frac{1}{2}$* .

The argument just presented is not quite waterproof, though. Firstly, it depends on the assumption of extreme initial anisotropy in the couplings, and secondly, it is based only on the leading-order scaling equations. As one scales towards larger couplings, sub-leading terms in the scaling equations can conceivably become important. Zaránd has investigated this issue by including next-to-leading-order logarithmic terms [generated by the diagrams in Fig. 7(b)] in the scaling equations, which turn out to be^{43,eq.(2.6)}:

$$\partial_x \underline{v}^A = -2i \sum_{BC} \varepsilon^{ABC} \underline{v}^B \underline{v}^C - 2N_f \sum_{B \neq A} \left[\underline{v}^A \text{Tr}[(\underline{v}^B)^2] - \underline{v}^B \text{Tr}[\underline{v}^A \underline{v}^B] \right] \quad (C9)$$

Note that the number of channels, N_f (equal to 2 for the case of interest), shows up here for the first time in the next-to-leading order, since each electron loop [see Fig. 7(b)] carries a factor N_f . Performing a careful analysis of the stability of the various fixed points that occur, he concluded that the above-mentioned $S_e = \frac{1}{2}$ fixed point is the only *stable* fixed point in of these equations.

Zaránd and Vladár also investigated the effect of the other channels, that don't couple as strongly as the two dominant ones, near the fixed point⁵⁰. They produce irrelevant operators that eventually scale to zero (which is why these channels decouple), but that can nevertheless influence the critical behavior near the fixed point. However, Zaránd and Vladár found that they have the *scale* critical exponent as the leading irrelevant operator in the pure 2CK model, which means that these extra operators don't change the universal critical behavior, merely some of the corresponding amplitudes.

Since these results are independent of the value of N_f and the number of orbital channels considered, and Zaránd's analysis is exact in the limit $N_f \rightarrow \infty$, he expects his results to also be valid for $N_f = 2$. (However, no completely rigorous proof exists yet for this expectation; in particular, his analysis assumes $\Delta_b = 0$, and the case $\Delta_b \neq 0$ is substantially more complicated, see^{9,(b),sectionIII}. For another, symmetry-based argument in favor of $S_e = \frac{1}{2}$, see^{45,section3.3.2(iii)}.)

4. The fixed point is Pseudo-Spin Isotropic

Next one shows, following^{43,section III}, that the $S_e = \frac{1}{2}$ fixed point is actually *isotropic* in pseudo-spin space.

The last term in Eq. (C9) can be eliminated from the fixed-point analysis by making a suitable orthogonal transformation $\underline{v}^A \rightarrow \sum_B O_{AB} \underline{v}^B$. Therefore, it is sufficient to consider the first two terms on the right-hand side of Eq. (C9). At the fixed point, where $\partial_x \underline{v}^A = 0$, we have

$$\sum_{BC} \varepsilon^{ABC} \underline{v}^B \underline{v}^C = i N_f \underline{v}_A \sum_{B \neq A} \text{Tr}[(\underline{v}^B)^2]. \quad (\text{C10})$$

Multiplying by \underline{v}^A and taking the trace, one obtains the three relations

$$i N_f \boldsymbol{\alpha}^A (\boldsymbol{\alpha}^B + \boldsymbol{\alpha}^C) = \boldsymbol{\beta}, \quad \text{where } \{A, B, C\} = \{x, y, z\} \quad (\text{cyclically}), \quad (\text{C11})$$

where we have defined $\boldsymbol{\alpha}^A \equiv \text{Tr}[(\underline{v}^A)^2]$ and $\boldsymbol{\beta} \equiv \text{Tr}(\underline{v}^A \underline{v}^B \underline{v}^C - \underline{v}^C \underline{v}^B \underline{v}^A)$. This immediately implies one of two possibilities: either at least two of the $\boldsymbol{\alpha}^A$'s are zero, which is the trivial (commutative) case without electron-assisted tunneling ($\underline{v}^x = \underline{v}^y = 0$); or else they are all equal:

$$\boldsymbol{\alpha}^A = \boldsymbol{\alpha}^B = \boldsymbol{\alpha}^C = \boldsymbol{\alpha}. \quad (\text{C12})$$

The latter case is the one of present interest. The conclusion that the couplings are all equal (i.e. the effective Hamiltonian isotropic) was checked numerically by Zaránd^{43, Fig. 4}, and is illustrated in Fig. 8.

What is the matrix structure of the \underline{v}^A 's? Introducing the notation $J^A = \frac{1}{2N_f} \boldsymbol{\alpha}^A \underline{v}^A$, Eqs. (C10) and (C12) imply that the J^A satisfy the $SU(2)$ Lie algebra,

$$[J^A, J^B] = i \varepsilon^{ABC} J^C, \quad (\text{C13})$$

which means that they must be a direct sum of irreducible $SU(2)$ representations:

$$J^A = \sum_{\oplus k=1}^n S_{(k)}^A. \quad (\text{C14})$$

According to the analysis of Zaránd mentioned in the previous section, only a single subspace $S_e = \frac{1}{2}$ in this sum corresponds to a stable fixed point (all the others correspond to unstable fixed points), in the vicinity of which we can therefore write $J_{\alpha\alpha'}^A = \frac{1}{2} \sigma_{\alpha\alpha'}^A$.

After a rotation in α -space to line up the quantization axis of the pseudospins of the impurity and the electrons, the effective Hamiltonian to which (B3) renormalizes can be written as:

$$H_{int} = \int d\varepsilon \int d\varepsilon' \sum_{\alpha\alpha'=1,2} \sum_{aa'=1,2} \sum_{i=\uparrow,\downarrow} v_K \left(c_{o\varepsilon\alpha i}^\dagger \frac{1}{2} \vec{\sigma}_{\alpha\alpha'} c_{o\varepsilon'\alpha' i} \right) \cdot \left(b_a^\dagger \frac{1}{2} \vec{\sigma}_{aa'} b_{a'} \right). \quad (\text{C15})$$

Here v_K is the magnitude of the effective tunneling center-electron coupling (and estimated^{42, Table 1} to be of order $v_K \simeq 0.1 - 0.2$). This is the main result of the RG analysis: *The effective Hamiltonian has exactly the form of the isotropic, magnetic 2-channel Kondo*

problem; the two surviving orbital indices $\alpha = 1, 2$ play the role of pseudo-spin indices and the Pauli spin indices $i = \uparrow, \downarrow$ the role of channel indices.

An intuitively appealing interpretation of this model, due to Moustakas and Fisher, is given in Appendix B, after Eq. (B10).

We conclude this appendix with a number of miscellaneous comments:

The fact that one always scales towards an *isotropic* effective Hamiltonian is rather remarkable (though in accord with the conformal field theory results that show that anisotropy is an irrelevant perturbation^{26,eq.(3.17)}): the initial extreme anisotropy of the couplings is dynamically removed, and a $SU(2)$ symmetry emerges that is not present in the original problem!

Note that the initial signs of the anisotropic coupling constants did not matter in the above arguments. A more careful argument^{45,section3.3.2(ii)} shows that the flow toward this fixed point indeed occurs irrespective of the initial signs of the coupling constants.

Relevant perturbations: When the initial splitting Δ_b is non-zero, the 2-nd order RG is considerably more complicated^{9,(b),sectionIII}. The result is that Δ_b gets normalized downward by about two orders of magnitude^{9,(b),Fig.3}. However, as emphasized in^{45,section3.4.1(c)}, *the splitting Δ_b is nevertheless a relevant perturbation*: it can be shown to scale downward much slower than the bandwidth D' , so that $\Delta_b(D')/D'$ grows as D' is lowered.

By analyzing the stability of the fixed point equations against a perturbation that breaks *channel* symmetry, it can likewise be shown that *channel anisotropy* is a relevant perturbation^{45,section3.4.1(c)}.

Kondo temperature: The Kondo temperature is the cross-over temperature at which the couplings begin to grow rapidly. It can be estimated from an approximate solution of the second order scaling equation (C9).²³ The result found for T_K by VZ^{9,p.1590,eq.(4.11)} is

$$T_K = D [v^x(0)v^z(0)]^{1/2} \left(\frac{v^x(0)}{4v^z(0)} \right)^{\frac{1}{4v^z(0)}}. \quad (\text{C16})$$

Note that the factor $[v^x(0)v^z(0)]^{1/2}$ is absent²⁴ if one estimates T_K only from the leading-order scaling equation (C3)^{9,p.1577,eq.(4.11)}. Since the bare $v^x(0) \ll 1$, this factor causes a substantial suppression of T_K (by about two orders of magnitude), if one simply inserts $v^x(0)$ into Eq. (C16), leading to pessimistically small values of $T_K \simeq 0.01 - 0.1$ K^{41,42}. However, the inclusion of excited states remedy this problem, in that excited states renormalize v^x to larger values by about two orders of magnitude (see below).

²³Since T_K is only a statement about the *onset* of rapid growth of coupling constants, the value obtained from scaling equations derived by perturbation theory is expected to give approximately the correct scale even though the scaling equations themselves become invalid when the couplings become too large⁵¹.

²⁴The presence of the prefactor to the exponent in (C16) is of course a well-known feature of second-order scaling, see e.g.^{55,eq.(3.47)}.

5. The Role of Excited States

Let us now return to the more general problem where the excited states in Eq. (B2) with energies E_{ex} , are not neglected from the beginning.

The first important consequence of including excited states in the model has already been discussed in section C 1: electron-assisted hopping transitions between the two wells *via excited states* allow Kondo physics to occur even if the barrier is so large that direct and electron-assisted tunneling through the barrier is negligible (i.e. $\Delta_o \simeq 0$). This is good news, since the energy splitting $\Delta_b = E_1 - E_2$ is limited from below by Δ_o , but simultaneously Δ_b (being a relevant perturbation) needs to be very small if scaling to the 2-channel fixed point is to take place.

Secondly, in the presence of excited states, poor man's scaling towards strong-coupling, based on Eq. (C3), has to proceed in several steps: the excited state $|\Psi_c\rangle$ only contributes as long as the effective bandwidth D' is larger than E_c , as is made explicit by the $\theta(D' - E_c)$ in Eq. (C3). As soon as $D' < E_c$, the excited state decouples.

Assuming that the presence of excited states does not affect the result found in section C 3, namely that the effective Hamiltonian scales towards a 2-D subspace in which the electrons have pseudo-spin $S_e = \frac{1}{2}$, Zar\'and and Zawadowski^{41,42} have analyzed the successive freezing out of excited states. They concluded that when D' becomes smaller than the smallest excited-state energy E_3 , one ends up with a tunneling center of formally precisely the same nature as the one discussed in sections C 3 and C 4, *but with renormalized couplings*.

The renormalized couplings turn out to be still small, which means that the perturbative scaling analysis of sections C 3 and C 4 still applies; however, v^x and v^y are renormalized upward by a factor of up to 50 from their bare values (which were three orders of magnitude smaller than v^z see Eq. (C1)). This has very important consequences for the Kondo temperature Eq. (C16), which strongly depends on v^x : with realistic choices of parameters (given in the caption to Fig. 1) the Kondo temperature turns out to be about 2 orders of magnitude larger with than without excited states in the model, and Kondo temperatures in the experimentally relevant range of 1 to 3 K were obtained^{42,tableII}.

To summarize: the inclusion of excited states in the model leads to more favorable estimates of the important parameters Δ_o (can be zero) and T_K (larger); but since the excited states eventually decouple for small enough effective band-widths, they do not affect the flow toward the 2-channel Kondo fixed point in any essential way.

APPENDIX D: RECENT CRITICISM OF THE 2-CHANNEL KONDO SCENARIO

Very recently, the claim that Zawadowski's non-magnetic Kondo problem will renormalize to the non-Fermi-liquid fixed point of the 2-channel Kondo model at sufficiently low temperatures has been called into question in two separate papers^{12,15}. We ignored the concerns stated there when introducing our NTKM in section II, because there our attitude was phenomenological and our aim merely to write down a phenomenological Hamiltonian that accounts for the observed phenomena. However, the question as to whether or not the bare non-magnetic Kondo model does indeed renormalize toward the non-Fermi-liquid fixed point 2CK model is an interesting theoretical one in its own right, which, in our view, has

become all the more relevant in the light of the apparent success of the NTKM in accounting for all aspects of RB's experimental results. Therefore, we summarize the relevant issues in this appendix.

1. Large Δ due to Static Impurities

Wingreen, Altshuler and Meir have recently argued¹² that tunneling centers with very small splittings ($\Delta < 1K$) can not occur at all in a disordered material if the TLS-electron coupling has the large values that apply to the over-screened 2-channel Kondo fixed point. Their argument goes as follows:

If H_{TC} of Eq. (B2) is truncated to the lowest two states and written in the left-right basis [see Eq. (C4)], it has the following general form: $H_{TC} = \frac{1}{2} \sum_{A=x,y,z} \Delta_A \sigma^A$, where Δ_z is the asymmetry energy and Δ_x the spontaneous hopping rate (for the bare system, time-reversal symmetry enables one to choose $\Delta_y = 0$ by choosing real eigenfunctions, but under renormalization $\Delta \neq 0$ can be generated, see below). Hence Δ_A can be interpreted as an effective local field at the TLS site (in the language of the magnetic Kondo problem, this would be called a local "magnetic field"). The energy splitting is of course $\Delta = (\Delta_x^2 + \Delta_y^2 + \Delta_z^2)^{1/2}$.

Now, WAM pointed out that ordinary elastic scattering of electrons off other static defects in the system, which causes Friedel oscillations (wavelength $1/k_F$) in the electron density (see e.g.⁵⁶), will make a random contribution to Δ_A (not considered in Zawadowski's theory). The magnitude of this effect can be characterized by the *typcial* $\bar{\Delta} = \langle \Delta^2 \rangle^{1/2}$, i.e. the average of Δ over all realizations of disorder.²⁵

WAM estimated $\bar{\Delta}$ using simple 2nd-order perturbation theory in the coupling between the electrons and static impurities, and found²⁶

$$\bar{\Delta} \simeq \varepsilon_F v_K / \sqrt{k_F \ell}. \quad (\text{D1})$$

Here ℓ is the mean free path (a measure of the concentration of static impurities), and v_K the effective TLS-electron coupling strength in Eq. (B10). Moreover, WAM argue that because Δ_A has three components, the probability distribution $P(\Delta)$ goes to 0 at $\Delta = 0$, because the probability to simultaneously find *all three* components $\Delta_A = 0$ is vanishingly small.

WAM estimated $v_K \simeq 0.1$ at the 2CK fixed point, by using a Kondo temperature of about 4K (as cited in⁶) in the standard formula $v_K = \log(k_B T_K / \epsilon_F)$ obtained from the leading-order scaling equations. (This value for v_K agrees with the values estimated by

²⁵Actually, $\bar{\Delta}$, the *average* of Δ over all realizations of disorder, can considerably overestimate the *typcial* splitting, because the average can be dominated by a few realizations of disorder that give rise to very large splittings (e.g. if some static defect is very close to the TLS, so that the Friedel oscillations have very large amplitudes at the TLS). However, following WAM, we shall nevertheless refer to $\bar{\Delta}$ as the typical splitting.

²⁶Cox has reproduced WAM's result⁵⁷ by a simple calculation analogous to the one by which one obtains the RKKY interaction between two magnetic impurities.

Zar\'and and Zawadowski⁴² for the 2CK fixed point (see caption of Fig. 1). Using $l \simeq 3$ nm, WAM then found a value of $\Delta \simeq 100K$ (the result is so large because according to Eq. (D1) $\bar{\Delta}$ is proportional to ε_F).

Since 100 K is a huge energy scale compared to all other scales of interest, WAM argued that the 2-channel Kondo physics evoked in paper I to explain the Ralph-Buhrman experiment would never occur. Instead, they proposed an alternative explanation of the experiment based on disorder-enhanced electron interactions. The latter suggestion, which we believe contradicts several experimental facts^{12,(b)}, is critically discussed section V A of paper I. Here we briefly comment on their estimate of $\bar{\Delta}$, following^{12,(b)} and¹⁶.

We believe that WAM are correct in pointing out that static disorder interactiond can act to increase the energy splitting, Δ , of the TLS. However, we suggest that $\bar{\Delta} \sim 100$ K may be a considerable overestimate, for the following reason.

According to Zar\'and and Zawadowski (ZZ)¹⁶, WAM's statements are equivalent to assuming that Δ_A is renormalized by Hartree-type corrections to the TLS self-energy (see Fig. 2 of¹⁶ for the Feynman diagram): $\Sigma_A(\omega) = \int d\omega \rho_{\alpha\alpha'}(\omega) \tilde{v}_{\alpha'\alpha}^A [\ln(\omega/D)]$. Here $\rho_{\alpha\alpha'}(\omega)$ is the spectral function of the conduction electrons in the presence of impurities and \tilde{v}^A the renormalized vertex function of Eq. (C4) [with $x = \ln(\omega/D)$ there; the corresponding bare vertex function would be $\tilde{v}^A(0)$]. WAM's estimate of $\bar{\Delta} = 100$ K is obtained if one simply uses the unrenormalized diagonal part of the spectral function. However, this is too simplistic, since if the renormalized spectral function is used, Δ_A is reduced significantly^{41,58} (despite the growth in the couplings \tilde{v}^A under renormalization). The spontaneous hopping rates Δ_x, Δ_y , in particular, *decrease* by as much as three orders of magnitude under renormalization (ZZ estimate their final typical value to be $\bar{\Delta}_x \simeq \bar{\Delta}_y \lesssim 1$ to 0.1 K¹⁶). This simply reflects the screening of the TLS by conduction electrons: when tunneling between the wells, the tunnling center has to drag along its screening cloud, which becomes increasingly difficult (due to the orthogonality catastrophe) at lower temperatures. In contrast, the asymmetry term Δ_z is not reduced as much⁵⁸ (ZZ estimate that after renormalization $\bar{\Delta}_z \gtrsim 1$ K), because of a much larger value of the bare coupling $\tilde{v}^z(0)$ [$\simeq 10^3 \tilde{v}^x(0) \simeq 10^3 \tilde{v}^y(0)$, see Eq. (C1)].

Thus, we believe that the reason for WAM's huge estimate of $\bar{\Delta} = 100$ K is their neglect of the reduction of Δ_A under scaling. Though ZZ's studies of this reduction were performed without considering static disorder, disorder should not essentially change matters²⁷ (since this reduction simply reflects the well-understood physics of screening). Moreover, because Δ_x, Δ_y end up being so much smaller than Δ_z , WAM's conclusion that $P(0) = 0$ for the distribution of splittings is not persuasive, because the distributions $P_A(\Delta_A)$ of the individual Δ_A are not equivalent, as they assumed.

Note that although $\bar{\Delta}_z \gtrsim 1$ K, implying that also $\bar{\Delta} \gtrsim 1$ K, this is only a statement about the *typical* splitting of a typical TLS. In a disordered system, it seems very likely that some TLSs will exist with a splitting Δ significantly smaller than the typical $\bar{\Delta}$. In particular, ZZ's estimate that typically Δ_x, Δ_y are $\lesssim 0.1$ K implies that assumption (A2) of paper I,

²⁷To check this statement, an extra term, including the effects of static disorder, should be added to Zawadowski's Hamiltonian, and then a full RG analysis should be performed to determine *self-consistently* how the couplings and the “local field” Δ_A , evolve together under renormalization.

section VID), namely that the nanoconstriction does contain TLS with $\Delta < 1$ K, does not seem unreasonable, despite the fact that $\bar{\Delta} \gtrsim 1$ K.

Finally, note that two-state systems with small energy splittings ($\Delta < 1$ K) have been directly observed in disordered metals in at least two experiments: Graebner *et al.*⁵⁹ found a linear specific heat in amorphous superconductors below T_c in the regime $0.1 < T \lesssim 2$ K, which they attributed to two-state systems; and Zimmerman *et al.* directly observed individual slow fluctuators in Bismuth wires^{60,61}, with Δ_s as small as 0.04 K. Though the detailed properties of these two-state systems may be different than those of fast TLS, this illustrates that even in systems where the average splitting is expected to be large, the physics *can* be sometimes dominated by those two-state systems that have smaller splittings.

The relevance of WAM's calculation to the interpretation of the experiments discussed in paper I are discussed in section VI C 3 of paper I.

2. Another Relevant Operator

The theoretical justification for the non-magnetic Kondo model proposed by Zawadowski has recently also been questioned by Moustakas and Fisher (MF)¹⁵. Reexamining a degenerate two-level system interacting with conduction electrons, they argued that the model of Eqs. (B6) and (B7) used by Zawadowski is incomplete, because it neglects certain subleading terms in the TLS-electron interaction that have the same symmetries as the leading terms. MF showed that when combined in certain ways, they generate an extra *relevant* operator, not present in Zawadowski's analysis, which in general prevents the system from flowing to the $T = 0$ fixed point. Therefore, unless a fine-tuning of parameters miraculously causes this relevant operator to vanish, it will eventually always become large, and the system will never reach the $T = 0$ fixed point.

Zawadowski *et al.*¹⁷ have recently investigated the nature of this new relevant term. Preliminary investigations suggest that it arises due to the breaking of particle-hole symmetry. They estimate that before renormalization, its prefactor in the bare model is smaller than the effective Kondo coupling at the fixed point by a factor of 10^{-6} , and still by 10^{-3} after poor man's scaling renormalization to effective bandwidths of order $D' = \Delta_o$ (the spontaneous tunneling rate). Thus, they conclude that this effect can probably be neglected in realistic systems. However, their conclusions are still preliminary and this issue deserves further investigation⁶².

APPENDIX E: THE LIMIT OF LARGE CHANNEL NUMBER: $K \rightarrow \infty$

In this appendix, we perform a check on the CFT calculation of the backscattering current of section V, by considering the (unphysical) limit of a large number of conduction electron channels, $i = 1, \dots, k$, with $k \rightarrow \infty$. In this limit, the poor man's scaling approach becomes exact, even though it is based on perturbation theory. The reason for this is that (for the isotropic model) the over-screened fixed point occurs when the coupling constant has the special value $v^* = \frac{2}{2+k}$ [see e.g. section II B of paper III for the case $k = 2$], which $\rightarrow 0$ as $k \rightarrow \infty$. Thus, in this limit one never scales into a “strong-coupling” regime, and the perturbative expressions from which the scaling equations are derived retain their validity

throughout. Therefore, results from the poor man's scaling approach should agree with exact results from CFT in the limit $k \rightarrow \infty$, which serves as a useful check on both methods.

Thus, in this appendix we consider the k -channel version of the NTKM of section II, in which the index $i = 1, \dots, k$, but the interaction still has the form of Eq. (8).

1. Backscattering current

To begin, we need a perturbative expression for the backscattering current ΔI (i.e. the negative contribution to I , which we defined such that $I > 0$ if it flows to the right) due to the backscattering events of $V_{\eta\eta'}^{aa'}$. We use the most naive approach for treating the effects of the interaction in a non-equilibrium situation: we simply do perturbation theory in H_{int} according to the rules of $T = 0$, $V = 0$ quantum mechanics, and insert by hand, into all sums over intermediate states, appropriate non-equilibrium distribution functions that indicate with what probability the corresponding states are occupied or empty, $\sum_\eta \int d\varepsilon f_\sigma(\varepsilon)$ or $\sum_\eta \int d\varepsilon [1 - f_\sigma(\varepsilon)]$, as in Eq. (B8). This is the method Kondo⁶³ used when deriving his famous $\log T$ for the first time, and when one is merely interested in the lowest few orders of perturbation theory, it is certainly the simplest approach.

In this approach, ΔI is given quite generally by²⁸

$$\Delta I = -\frac{\tilde{K} N_o}{|e|} \int d\varepsilon \int d\varepsilon' \left[b_{\eta\eta'} (1 - f_\sigma(\varepsilon)) f_{\sigma'}(\varepsilon') \Gamma(\varepsilon', \sigma' \rightarrow \varepsilon, \sigma) \right. \quad (E1)$$

$$\left. - b_{\eta'\eta}^* (1 - f_{\sigma'}(\varepsilon')) f_\sigma(\varepsilon) \Gamma(\varepsilon, \sigma \rightarrow \varepsilon', \sigma') \right] , \quad (E2)$$

where $\sigma = L$ and $\sigma' = R$, and the backscattering rate from σ' -movers to σ -movers is

$$\Gamma(\varepsilon', \sigma' \rightarrow \varepsilon, \sigma) = 2\pi/\hbar \delta(\varepsilon' - \varepsilon) N_o^{-2} \frac{1}{2} \sum_{\alpha i a, \alpha' i' a'} |T_{\varepsilon\eta\varepsilon'\eta'}^{aa'}|^2 . \quad (E3)$$

In writing down Eq. (E1), the fact that the Fermi functions do not depend on the indices that appear in the sums $\sum_{\alpha i a, \alpha' i' a'}$ has been exploited to pull them out to the front of these sums, which could thus be included in the definition (E3) of Γ . In Eq. (E3) the factor $\frac{1}{2}$ has been included so that $\frac{1}{2} \sum_{a'}$ represents an average over the initial states of the TLS. $T_{\varepsilon\eta\varepsilon'\eta'}^{aa'}$ is the generalization of the interaction vertex $\Gamma_{\eta\eta'}^{aa'}$ of Eq. (B8) to all orders of perturbation theory, and depends not only on the matrix elements $V_{\eta\eta'}^{aa'}$, but also on the distribution functions $f(\varepsilon, \eta)$ (as Eq. (B8) illustrates explicitly). The factor $\tilde{K} \equiv e^2 \sum_\eta \tau_\eta(0)/h$ (where $\tau_\eta(\varepsilon)$ is defined below) is included in Eq. (E1) for dimensional reasons, and the dimensionless constants $b_{\eta\eta'}$ characterize all those details of scattering by the impurity that are energy-independent and of a sample-specific, geometrical nature, such as the position of the impurity relative to the constriction, etc. (compare section III of paper I).

Now, since $V_{\eta\eta'}^{aa'}$ is independent of the indices σ, σ' , the same is true for $|T_{\varepsilon\eta\varepsilon'\eta'}^{aa'}|^2$. (Although the “internal sums” $\sum_{\sigma''}$ involving intermediate states are highly non-trivial, because

²⁸Though the relation of the perturbative expression (E1) to the non-perturbative ones of section V is not readily apparent, note that Eq. (E5) has the same form as Eq. (53).

of the presence of σ'' -dependent $f(\varepsilon\eta'')$ functions, $T_{\varepsilon\eta\varepsilon'\eta'}^{aa'}$ of course does not depend on such σ'' -indices, since they are summed over.) Therefore it follows immediately that

$$\Gamma(\varepsilon', \sigma' \rightarrow \varepsilon, \sigma) = \Gamma(\varepsilon, \sigma \rightarrow \varepsilon', \sigma') . \quad (\text{E4})$$

Exploiting eq. (E4) and the $\delta(\varepsilon' - \varepsilon)$ function in $\Gamma(\varepsilon', \sigma' \rightarrow \varepsilon, \sigma)$, the backscattering current can be brought into the suggestive form [compare with Eq. (53)]

$$\Delta I = -\frac{\tilde{K}b}{|e|} \int d\varepsilon' [f_R(\varepsilon') - f_L(\varepsilon')] \frac{1}{2} \sum_{\alpha', i'} \frac{1}{\tau_{\eta'}(\varepsilon')} . \quad (\text{E5})$$

Here we have taken $b_{\eta\eta'} = b$ for simplicity, and have defined the total scattering rate $\frac{1}{\tau_{\eta'}(\varepsilon')}$ for a electron with energy ε' and discrete quantum numbers η' by²⁹

$$\frac{1}{\tau_{\eta'}(\varepsilon')} \equiv N_o^{-1} \int d\varepsilon \sum_{\eta} \frac{2\pi}{\hbar} \delta(\varepsilon' - \varepsilon) \frac{1}{2} \sum_{aa'} |T_{\varepsilon\eta\varepsilon\eta'}^{aa'}|^2 . \quad (\text{E6})$$

How is $T_{\varepsilon\eta\varepsilon\eta'}^{aa'}$ to be calculated explicitly? For $T > T_K$, the leading order logarithmic terms of the perturbation series in powers of H_{int} can be summed up using the poor man's scaling approach, discussed in the next subsection. On the other hand, an analysis of the regime around the $T = 0, V = 0$ fixed point requires the use of CFT (see paper III). A consistency check between the two methods can be performed by taking the limit $k \rightarrow \infty$ in which perturbation theory becomes exact, as discussed above.

2. Gan's Results for Large Channel Number

A calculation of $\tau_{\eta}^{-1}(\varepsilon)$ for the bulk isotropic k -channel Kondo model, in the limit $k \rightarrow \infty$, has been carried out by Gan⁶⁴. More specifically, he calculated the imaginary part of the electron self-energy, $\Sigma^I(\omega, D, g)$, perturbatively³⁰ to order k^{-4} (we cite only the lowest relevant terms below). By then using poor man's scaling methods, he was able to obtain agreement to order k^{-2} with the exact CFT results for Σ^I .

Since Gan considered precisely the interaction Hamiltonian of Eq. (12) that governs our even channels, we can directly use his results. He obtained the following expression at $T = 0, V = 0$:

$$\Sigma^I(\omega, D, v_K) \propto \left[1 - c_1 \left(\frac{\omega}{T_K} \right)^{\bar{\alpha}} \right] . \quad (\text{E7})$$

²⁹The $\frac{1}{2}$ in Eq. (E5) is needed because the definition (E6) of $\tau_{\eta'}^{-1}$ contains a sum $\sum_{\sigma'}$ that does not occur in Eq. (E3), and is = 2, since $T_{\eta\eta'}^{aa'}$ is independent of σ' .

³⁰Since the coupling constant $v \sim 1/k$, and closed electron loops get a factor k , Gan had to include up to 8-th order diagrams!

His perturbative expression for the exponent occurring here is $\bar{\alpha} = \frac{2}{k}(1 - \frac{2}{k})$, which agrees to order k^{-2} with the exact CFT result $\alpha = \frac{2}{2+k}$.

Since Eq. (E7) was derived using poor man's scaling methods, *it also holds in the non-equilibrium case*, as long as $\omega > V$ (see section II E). This condition does not hold strictly in the integral (E5). Nevertheless, if we use $\frac{1}{\tau(\omega)} = -2\Sigma^I(\omega)$ in Eq. (E5) with $T = 0$, $V \neq 0$, the resulting asymptotic expression for the backscattering conductance $\Delta G(V, 0) = \partial_V \Delta I(V, 0)$,

$$\Delta G(V, 0) \propto V^{\bar{\alpha}}, \quad (E8)$$

should still be approximately correct up to logarithmic corrections that are typical of the poor man's scaling approach. Indeed, the corresponding expression that we obtained in section V from our CFT approach has the same asymptotic form [see Eq. (58)], but with $\bar{\alpha}$ replaced by the exact value for the exponent, namely $\alpha = \frac{2}{2+k}$. [Actually, in section V we always use $k = 2$, and hence $\alpha = \frac{1}{2}$ in Eq. (58).] This agreement is a reassuring confirmation that the methods used in sections III to V agree with the present perturbative results in the one limit ($k \rightarrow \infty$) where perturbation theory can be trusted.

APPENDIX F: HERSHFIELD'S Y -OPERATOR APPROACH TO NON-EQUILIBRIUM PROBLEMS

In this appendix we summarize the main ideas of Hershfield's Y -operator approach to non-equilibrium problems.

1. The Kadanoff-Baym Ansatz for $V \neq 0$

The problem at hand is defined by the free Hamiltonian H_o of Eq. (2), the free density matrix ρ_o of Eq. (4) and the interaction H_{int} of Eq. (8). H_o and ρ_o describe free electrons that move between two leads or baths (R/L), at different chemical potentials (μ_{\pm}), by passing ballistically through a nanoconstriction, in which L - and R -movers can be scattered into each other by H_{int} .

How does one calculate statistical averages for such a system, in other words, how does one define the full density matrix in the presence of H_{int} ? The main complication that has to be confronted is that the number of electrons in each bath is not conserved, in that $[N_{L,R}, H_{int}] \neq 0$ (compare footnote 6 on page 8). Therefore, any attempt to naively replace $\rho_o(V)$ in Eq. (4) by $e^{-\beta(H - Y_o)}$ will (apart from lacking first-principles justification) quickly run into problems: since $[H, Y_o] \neq 0$, many of the standard properties of equilibrium Green's functions [e.g. $G(\tau + \beta) = \pm G(\tau)$], no longer hold.

Kadanoff and Baym have shown how such a general problem can be dealt with, by using the notion of adiabatically switching on the interaction^{18,eq.(6.20)}: Thermal weighting has to be done with the initial density matrix ρ_o at some early time $t_o \rightarrow -\infty$, at which all interactions H_{int} are switched off, and then H_{int} is adiabatically turned on [$H_{int}(t) \equiv H_{int}e^{\alpha t}$, with $\alpha \rightarrow 0^+$] while the system is time-evolved to the time t of interest. Concretely, to evaluate the thermal expectation of an operator O , one writes the operator in the Schrödinger picture, and uses the thermal weighting factors $e^{-\beta[E_{on} - \frac{1}{2}eV(N_L - N_R)]}$ appropriate to a trace $\sum_n \langle n, t_o | | n, t_o \rangle$ of Schrödinger states taken at some early time $t_o \rightarrow -\infty$ (where they are

eigenstates of H_o with eigenvalues E_{on}). However, one then takes the actual trace between the *time-evolved versions* of these states $|n, t\rangle = U(t, t_o)|n, t_o\rangle$, where³¹ $U = e^{-iH(t-t_o)}$ is the Heisenberg time-evolution operator:

$$\langle O(t) \rangle_V \equiv \frac{\sum_n e^{-\beta[E_o - \frac{1}{2}eV(N_L - N_R)_n]} \langle n, t | O | n, t \rangle}{\sum_n e^{-\beta[E_{on} - \frac{1}{2}eV(N_L - N_R)_n]}} = \frac{\text{Tr} \rho_o(V, t_o) U^\dagger(t, t_o) O U(t, t_o)}{\text{Tr} \rho_o(V, t_o)}, \quad (\text{F1})$$

where in the second equality the trace is taken between the states $|n, t_o\rangle$. (Since steady-state expectation values of a single operator are time-independent, t is here just a dummy variable, and is often taken to be 0.)

Eq. (F1) is the defining prescription for taking non-equilibrium expectation values in the presence of interactions. For $V = 0$, it reduces to the standard equilibrium prescription,³²

$$\langle O \rangle_{V=0} \equiv \frac{\text{Tr} \rho(0, t_o) O}{\text{Tr} \rho(0, t_o)}, \quad \text{where} \quad \rho(0, t_o) \equiv e^{-\beta H}, \quad (\text{F2})$$

as shown, e.g., by Hershfield in¹⁴. Eq. (F2) is of course the starting point for familiar equilibrium statistical mechanics. One of its most useful features is that the thermal weighting factor $e^{-\beta H}$ and the dynamical time-evolution factor $U(t, t_o) = e^{-iH(t-t_o)}$ commute; Green's functions therefore have the periodicity property $G(\tau + \beta) = \pm G(\tau)$, which makes it convenient to formulate perturbation expansions in H_{int} along the negative imaginary axis, $t = -i\tau \in [0, -i\beta]$.

2. Hershfield's Formulation of the case $V \neq 0$

If $V \neq 0$ so that Eq. (F1) and not Eq. (F2) is the starting point, there are no obvious periodicity properties along the imaginary time axis, and the conventional approach, due to Keldysh, is to formulate perturbation expansions in H_{int} along the real axis^{65,66}. The various non-equilibrium diagrammatic techniques that have been devised are simply ways of doing the real-time integrals $\int_{t_o}^t dt'$ that result from the expansion of $U(t, t_o)$. However, for our purposes such expansions are inconvenient: firstly, perturbation expansions have limited use in the Kondo problem, and secondly, we would in the end like to apply Affleck and Ludwig's non-perturbative CFT results.

Hershfield has recently shown that Eq. (F1) can be rewritten in a way that exactly meets our needs. The first step is trivial: using the cyclical property of the trace to move $U(t, t_o)$ to the front, Eq. (F1) can be written as

$$\langle O(t) \rangle_V \equiv \frac{\text{Tr} \rho(V, t) O}{\text{Tr} \rho(V, t)}, \quad (\text{F3})$$

³¹No time-ordered exponential is needed here, because H is assumed to be time-independent.

³²The second argument t_o in $\rho(0, t_o)$ is superfluous; it is retained here only for the sake of notational consistency with the $V \neq 0$ case.

where

$$\frac{\rho(V, t)}{\text{Tr}\rho(V, t)} \equiv \frac{U(t, t_o)\rho_o(V, t_o)U^\dagger(t, t_o)}{\text{Tr}\rho_o(V, t_o)} . \quad (\text{F4})$$

The formal definition (F4) makes it clear that $\rho(V, t)$ is the density operator that $\rho_o(V, t_o)$ develops into as the interaction is switched on and the system time-evolves from t_o to t , with appropriately changing normalization. Thus, all complications introduced through the adiabatic switch-on procedure are lumped into the time-evolved density operator $\rho(V, t)$.

Next, Hershfield transfers these complications to a new operator, Y , which he defines by writing $\rho(V, t)$ in the form

$$\rho(V, t) \equiv e^{-\beta[H-Y(V, t)]} , \quad (\text{F5})$$

purposefully constructed to resemble the definition of $\rho_o(V, t_o)$ in Eq. (4). Then he was able to show³³ (and herein lies the hard work) that the operator Y thus defined can be characterized as follows:

(P) Y is the operator into which Y_o evolves as the interactions are turned on [as is suggested by a comparison of Eqs. (F4) and (4)]. It satisfies the relation

$$[Y, H] = i\alpha(Y_o - Y) , \quad \text{where } \alpha \rightarrow 0^+ , \quad (\text{F6})$$

which implies that Y is a conserved quantity.

The fact that the Y -operator is a conserved quantity is the great advantage of the Y -operator approach. It implies that the problem is now formally equivalent to an equilibrium one (for which one has μN (N = total electron number) instead of Y , and $[H, N] = 0$).

Once the scattering states have been found, one can therefore apply the usual methods of equilibrium statistical mechanics,³⁴ using the density matrix $\rho \equiv e^{-\beta(H-Y)}$ and Heisenberg time-development $\hat{O}(\tau) = e^{H\tau}\hat{O}e^{-H\tau}$, to calculate physical quantities.

Explicit expressions for H and Y in a typical scattering problem are given in section III A.

³³Hershfield's proof is perturbative: using Eq. (F6) he showed explicitly that Eq. (F5), expanded in powers of H_{int} , reproduces the Keldysh perturbation expansion obtained from the Kadanoff-Baym Ansatz (F1).

³⁴From Eq. (14) it is clear that Y can actually be shifted away in $\rho = e^{-\beta(H-Y)}$ by defining new energies $\varepsilon' \equiv \varepsilon - \mu_\eta$ associated with $c_{\varepsilon\eta}$, i.e. measuring the energy of an excitation relative to the Fermi surface of the bath from which it originates. The weighting factor then completely resembles its equilibrium form, but because $c_{\varepsilon\eta}(\tau) = c_{\varepsilon\eta}e^{-\tau(\varepsilon' + \mu_\eta)}$, extra factors of $e^{\pm\tau 2\mu_\eta}$ appear on some operators that are not diagonal in σ , such as H_{int} . We shall not follow this approach here.

APPENDIX G: EXAMPLE: 2-SPECIES POTENTIAL SCATTERING

In this appendix we illustrate the formalism developed in section IV D by applying it to a very simple scattering problem, namely the scattering of only two species of (spinless) electrons off a static scattering potential. We take η equal to the species index, $\eta \equiv \sigma = (L, R) = (+, -)$ (i.e. η contains no extra channel indices i , and L/R denotes physical L/R movers). As Hamiltonian we take [compare Eqs. (23) and (24)]:

$$H = H_o + H_{int} = \sum_{\sigma} \int \frac{dx}{2\pi} \psi_{\sigma}^{\dagger}(ix) (\delta_{\sigma\sigma'} i\partial_x + 2\pi\delta(x)V_{\sigma\sigma'}) \psi_{\sigma'}(ix') . \quad (\text{G1})$$

Here $V_{\sigma\sigma'}$ is simply a hermitian 2×2 matrix representing potential scattering of the two species into each other (i.e. the impurity is not a dynamical object with internal degrees of freedom). Since $V_{\sigma\sigma'}$ is Hermitian, we can make a unitary transformation of the form

$$\bar{\psi}_{\sigma} \equiv M_{\sigma\sigma'} \psi_{\sigma'} , \quad (\text{G2})$$

with M chosen such that it diagonalizes

$$H_{\text{scat}} = \sum_{\sigma\sigma'} \bar{\psi}_{\sigma}^{\dagger}(0) (MVM^{-1})_{\sigma\sigma'} \bar{\psi}_{\sigma'}(0) \equiv \bar{\psi}_{\sigma}^{\dagger}(0) (v_o \frac{1}{2} \delta_{\sigma\sigma'} + v_3 \frac{1}{2} \sigma_{\sigma'}^3) \bar{\psi}_{\sigma'}(0) . \quad (\text{G3})$$

Since the scattering term is now diagonal, its only effect on the $\bar{\psi}_{\sigma}$ -fields can be to cause a phase shift of the outgoing fields relative to the incident ones:

$$\bar{\psi}_{R\sigma}(ix) = P_{\sigma\sigma'} \bar{\psi}_{L\sigma'}(ix) \quad \text{for } x < 0 , \quad \text{where} \quad P_{\sigma\sigma'} = \delta_{\sigma\sigma'} e^{-i(\phi_o + \sigma\phi_3)} . \quad (\text{G4})$$

and the phase shifts ϕ_0 and ϕ_3 are functions of v_o and v_3 . Rotated back into the ψ_{σ} -basis, this phase shift of course becomes an actual $[SU(2)]$ rotation of the two species into each other:

$$\psi_{R\sigma}(ix) = \tilde{U}_{\sigma\sigma'} \psi_{L\sigma'}(ix) , \quad (\text{G5})$$

where $\tilde{U}_{\sigma\sigma'}$ is a unitary matrix of the form:

$$\tilde{U}_{\sigma\sigma'} \equiv (M^{-1}PM)_{\sigma\sigma'} \equiv \begin{pmatrix} \mathcal{T} & \mathcal{R} \\ -\mathcal{R}^*/\mathcal{T}^* & \mathcal{T} \end{pmatrix} , \quad [|\mathcal{T}|^2 + |\mathcal{R}|^2 \equiv 1] . \quad (\text{G6})$$

Comparing Eq. (G5) with Eq. (34) and Eq. (31), we see that $\tilde{U}_{\sigma\sigma'}(\varepsilon') = \tilde{U}_{\sigma\sigma'}$, i.e. in this simple case \tilde{U} is ε' -independent. Physically, this rotation of physical L - and R -movers into each other simply reflects the fact that H_{int} causes backscattering: an incoming L -mover has amplitude \mathcal{T} to undergo forward scattering and emerge as a L -mover, and \mathcal{R} to be backscattered into a R -mover. This illustrates how our formalism is able to deal with backscattering despite the fact that we expressed both $\sigma = L$ and $\sigma = R$ as mathematical L -movers in Eq. (20), for which both the transmitted (\mathcal{T}) and reflected (\mathcal{R}) parts of ψ_{σ} live at $x < 0$.

To calculate the current, insert Eq. (G6) into Eq. (40). One readily finds

$$I = \frac{|e|}{h} \sum_{\bar{\sigma}} \int d\bar{\varepsilon} |\mathcal{T}|^2 \bar{\sigma} f(\bar{\varepsilon}, \bar{\sigma}) = \frac{e^2}{h} |\mathcal{T}|^2 |V| . \quad (\text{G7})$$

As expected, the conductance $G \equiv \partial_V I = \frac{e^2}{h} |\mathcal{T}|^2$ is reduced from its customary value for a single channel in the absence of scattering, namely $\frac{e^2}{h}$, by the transmission coefficient squared $|\mathcal{T}|^2$.

Eq. (G7) can also be used to illustrate that the conductance assumes a *V/T scaling* form if the transmission coefficient \mathcal{T} is *energy dependent*. Assume that for some reason the \mathcal{T} in Eq. (G7) depends on the energy distance from the Fermi surface, and can be expanded as $|\mathcal{T}|^2 \equiv A_o + (\varepsilon/\varepsilon_F) A_1 + (\varepsilon/\varepsilon_F)^2 A_2 + \dots$. Then the conductance $G = \partial_V I$ is readily found to be

$$G(V, T) = \frac{e^2}{h} \left[A_o + A_2 \frac{\pi^2}{3} \left(\frac{T}{\varepsilon_F} \right)^2 \left(1 + \frac{3}{4\pi^2} \left(\frac{eV}{T} \right)^2 \right) \right]. \quad (\text{G8})$$

This has the scaling form $G(V, T) = G(0, 0) + BT^2\Gamma(v)$, where $\Gamma(v) = \left(1 + \frac{3}{4\pi^2}v^2 \right)$ is a universal function, and $v \equiv eV/T$.

In the 2CK case, a scaling form for the conductance arises in a similar fashion, namely from an energy-dependence in the transmission coefficient. The non-trivial difference is that there we shall find $|\mathcal{T}(\varepsilon)|^2 = A_o + A_1 T^{1/2} \tilde{\Gamma}(\varepsilon/T)$, see section V.

APPENDIX H: THE NCA APPROACH

In section VI we compare our results to recent numerical calculations by Hettler, Kroha and Hershfield (HKH)¹³, who used the non-crossing-approximation (NCA) approach to the Kondo problem. Therefore, a few words about their work are in order here.

1. Anderson model used for NCA

HKH represent the system by the following infinite- U Anderson Hamiltonian in a slave boson representation:

$$H_1 = \sum_{p,\sigma,\alpha,i} (\varepsilon_p - \mu_\sigma) c_{p\sigma\alpha i}^\dagger c_{p\sigma\alpha i}^\dagger + \varepsilon_d \sum_\alpha f_\alpha^\dagger f_\alpha + \sum_{p,\sigma,\alpha,i} \mathcal{V}_\sigma (f_\alpha^\dagger b_i c_{p\sigma\alpha i} + \text{H.c.}) . \quad (\text{H1})$$

The first term describes conduction electrons in two leads, $\sigma = (L, R) = (+, -)$, separated by a barrier and at chemical potentials $\mu_\sigma = \mu + \sigma \frac{1}{2}eV$. The electrons are labeled by a momentum p , the lead index σ , a pseudospin index $\alpha = (1, 2)$, and their Pauli spin $i = (\uparrow, \downarrow)$. The barrier is assumed to contain an impurity level ε_d far below the Fermi surface, hybridizing (with matrix elements \mathcal{V}_σ , with $\mathcal{V}_L = \mathcal{V}_R$ for our purposes) with the conduction electrons, which can get from one lead to the other only by hopping via the impurity level. f and b are slave fermion and slave boson operators, and the physical electron operator on the impurity is represented by $d_\alpha^\dagger b_i$, supplemented by the constraint $\sum_\alpha f_\alpha^\dagger f_\alpha + \sum_i b_i^\dagger b_i = 1$.

Although this picture of two disconnected leads communicating only via hopping through an impurity level does not directly describe the physical situation of ballistic transport through a hole accompanied by scattering off two-level systems, the Hamiltonian (H1) can be mapped by a Schrieffer-Wolff transformation onto the more physical one [Eq. (8)] introduced in section II A. It is therefore in the same universality class and describes the same

low-energy physics, provided that one identifies the impurity-induced “tunneling current” I_{tun} in the HKH model with the impurity-induced backscattering current ΔI in the actual nanoconstriction.

HKH calculate the tunneling current,

$$I_{tun}(V, T) = \int d\omega A_d(\omega) [f_o(\omega - eV/2) - f_o(\omega + eV/2)], \quad (H2)$$

where $f_o(\omega) = 1/(e^{\beta\omega} + 1)$, by calculating the impurity spectral function $A_d(\omega)$ using the NCA approximation, generalized to $V \neq 0$ using Keldysh techniques. The NCA technique⁶⁷ is a self-consistent summation of an infinite set of selected diagrams (which becomes exact in the limit $N \rightarrow \infty$, where N is the number of values the pseudo-spin quantum number can assume), and in that sense it is not an “exact” solution of the model. However, it has been shown³¹ that for a $U(1) \times SU(N)_s \times SU(M)_f$ Kondo model (i.e. M channels of electrons, each with N possible pseudo-spin values, here we have $N = M = 2$), the NCA approach gives leading critical exponents for $A_d(\omega)$ *identical* to those of conformal field theory for *all* N and M (with $M > 2$). Hence the NCA method can be regarded as a useful interpolation between the high- T regime where any perturbative scheme works, and the low- T regime where it gives the correct exact critical exponents. Moreover, when combined with the Keldysh technique, it deals with the non-equilibrium aspects of the problem in a more direct way than our CFT approach (it can be regarded as a self-consistent determination of the scattering amplitudes), and is able to go beyond the weakly non-equilibrium regime ($V \ll T_K$).

2. Electron Self-Energy

One would expect that the most direct comparison between CFT and the NCA could be obtained by comparing the retarded self-energy $\Sigma^R(\omega)$ for conduction electrons at $V = 0$, calculated from the NCA with that from CFT [essentially the function $\tilde{\Gamma}(x)$ of Eqs. (48) and (59)]. However, the usefulness of this comparison is somewhat diminished by the fact that the NCA self-energy is not a symmetric function of frequency, which is a result of using the asymmetric Anderson model. This asymmetry disappears when calculating the conductance, because $I_{tun}(V) = I_{tun}(-V)$ in Eq. (H2) even if $A_d(\omega) \neq A_d(\omega)$, meaning that the zero-bias conductance is the more meaningful quantity to compare (see next section). Nevertheless, for $\omega < 0$, the CFT and NCA results agree very well³⁰.

3. Impurity Spectral Function $A_d(\omega)$

Figure 9 is very instructive, in that it illustrates what when $eV \gg T_K$ (a regime not accessible to CFT), the Kondo resonance splits into two (as also found in⁶⁸ for a related model). (T_K is defined as the width at half maximum of the $V = 0$ impurity spectral function at the lowest calculated T .) However, note that even for $V \simeq T_K$, this splitting has not yet set in, illustrating that non-equilibrium effects are not important for $eV < T_K$. This is the main justification for the the approach followed in section III B of neglecting all V/T_K corrections to the scattering amplitudes.

APPENDIX I: V -DEPENDENT CORRECTIONS TO $\tilde{U}_{\eta\eta'}$

In this appendix, V -dependent corrections to the scattering amplitudes $\tilde{U}_{\eta\eta'}$ are discussed.

A key assumption made throughout this paper was that the scattering amplitudes that describe scattering in the non-Fermi-liquid regime are V -independent, for reasons given in section III B. However, a simple poor man's scaling argument shows that this assumption can not be correct in general: If $V > T$, then the RG flow will eventually be cut off at an energy scale of order V ; in the poor man's RG approach, this is implemented by replacing the renormalized bandwidth D' by V in the effective interaction vertex, which means that the effective renormalized Hamiltonian now is explicitly V -dependent, which means that the same will be true for its scattering amplitudes.

Intuitively, the V -dependence arises because when $V \neq 0$, the difference in Fermi energies of the L - and R leads causes the Kondo peak in the density of states to split^{69,68} into two separate peaks (at energies $\mu \pm \frac{1}{2}eV$, (see Fig. 9 of appendix H, taken from³⁰)). However, in the non-Fermi-liquid regime, this V -dependence can nevertheless be neglected, because when $V/T_K \ll 1$, the splitting of the Kondo peak by eV is negligible compared to its width, which is $\propto T_K$ (said differently, then $V \neq 0$ cuts off the RG flow at a point sufficiently close to the non-Fermi-liquid fixed point that the latter still governs the physics).

To investigate the onset of Kondo peak-splitting effects with increasing V but still in the non-Fermi-liquid regime, we use the same kind of arguments as the ones used by AL to find the leading T/T_K term in $G_{\eta\eta'}$ (see sections II C 2 and II C 3 of paper III): $V \neq 0$ breaks a symmetry of the system (namely $\sigma = L \leftrightarrow R$), and the breaking of a symmetry allows boundary operators to appear in the action describing the neighborhood of the fixed point that had been previously forbidden (for extensive applications of this principle, see^{26, section III.C}).

To find the form of the leading $V \neq 0$ boundary operator, we argue as follows: V enters the formalism only via Y_o [see Eq. (5)], which takes the following form when written in terms of the fields ψ_η of Eq. (20) or $\bar{\psi}_\eta$ of Eq. (26):

$$Y_o = \frac{1}{2}eV \sum_{\eta} \int_{-\infty}^{\infty} \frac{dx}{2\pi} \psi_\eta^\dagger(ix) \sigma \psi_\eta(ix) , \quad (I1)$$

$$= \frac{1}{2}eV \sum_{\bar{\alpha}\bar{i}} \int_{-\infty}^{\infty} \frac{dx}{2\pi} \left[\bar{\psi}_{e\bar{\alpha}\bar{i}}^\dagger(ix) \bar{\psi}_{o\bar{\alpha}\bar{i}}(ix) + \bar{\psi}_{o\bar{\alpha}\bar{i}}^\dagger(ix) \bar{\psi}_{e\bar{\alpha}\bar{i}}(ix) \right] . \quad (I2)$$

[For the second line we used $(N\sigma^z N^{-1})_{\bar{\sigma}\bar{\sigma}'} = \sigma_{\bar{\sigma}\bar{\sigma}'}^x$, with N given by Eq. (10).] Eq. (I2) shows that Y_o mixes even and odd channels. Since the CFT solution was formulated only in the even sector, the present model³⁵ can strictly speaking not be solved exactly by CFT for $V \neq 0$, unless one neglects all effects of Y_o on the fixed point physics.

The form (I2) for Y_o leads us to conjecture that the leading boundary operator appearing

³⁵However, related models exist which can be treated exactly by CFT even if $V \neq 0$, for example the model used by Schiller and Hershfield in⁷⁰. There, the pseudospin index is also the L - R index

in the action when $V \neq 0$ will have the form³⁶

$$\delta S_V = \lambda_{10} \frac{V}{T_K} \sum_{\bar{\alpha}\bar{i}} \int_0^\beta d\tau \left[\bar{\psi}_{e\bar{\alpha}\bar{i}}^\dagger(\tau) \bar{\psi}_{o\bar{\alpha}\bar{i}}(\tau) + \bar{\psi}_{o\bar{\alpha}\bar{i}}^\dagger(\tau) \bar{\psi}_{e\bar{\alpha}\bar{i}}(\tau) \right] \equiv \lambda_{10} \frac{V}{T_K} \int_0^\beta d\tau J_{eo}(\tau). \quad (\text{I3})$$

Since the “even-odd” current J_{eo} defined on the right-hand-side has scaling dimension 1 (i.e. $\bar{\alpha}_1 = 1, \alpha_0 = 0$), δS_V has scaling dimension zero (see Eq. (20) of paper III), and is therefore a marginal perturbation. This means that even if $V/T_K \ll 1$, if T/V is made sufficiently small the system will eventually flow away from the non-Fermi-liquid fixed point, at a cross-over temperature T_V^* , say. However, since this perturbation is marginal, it only grows logarithmically slowly as T is decreased, so that T_V^* will be *very* small. Therefore, the non-Fermi-liquid regime, in which one has both $V, T \ll T_K$ and $T > T_K$, can be rather large. The lack of deviations from scaling in the data for the low- T regime (see section VII of paper I) indicate that T_V^* is smaller than the lowest temperatures obtained in the experiment.

How does δS_V affect the scattering amplitudes? First note that the V -dependence of δS_V enters in a very simple way, namely as a “parameter” that governs the strength of the perturbation. Therefore, the methods of section IVD, which extract $\tilde{U}_{\bar{\eta}\eta}(\varepsilon)$ from an *equilibrium* CFT Green’s function, are still applicable.

Standard CFT arguments³⁷ show that the effect of δS_V on $\bar{G}_{\bar{\eta}\bar{\eta}'}$ is to simply cause a rotation of the $\bar{\sigma} = e/o$ indices of the outgoing $\bar{\eta}$ -fields relative to the incident $\bar{\eta}'$ -fields by

(i.e. the interaction matrix elements are $\frac{1}{2}\vec{\sigma}_{\sigma\sigma'} \cdot \vec{S}$), which means that

$$Y_o = \frac{1}{2}eV \sum_{\alpha i} \int_{-\infty}^{\infty} \frac{dx}{2\pi} \psi_{\alpha i}^\dagger(ix) \sigma_{\alpha\alpha'}^z \psi_{\alpha'i}(ix) = eV \int_{-\infty}^{\infty} \frac{dx}{2\pi} J_s^z(ix)$$

where \vec{J}_s is the spin current (see Eq. (4) of paper III). Now, in this case it is easy to find the exact Y -operator in the presence of the Kondo interaction. Y must both commute with H and reduce to Y_o when the interaction is switched off. This is evidently satisfied by $Y = eV \int_{-\infty}^{\infty} \frac{dx}{2\pi} \mathcal{J}_{sL}^z$, where \mathcal{J}_{sL}^z is the z-component of the new spin current $\vec{\mathcal{J}}_s(ix) = \vec{J}_s(ix) + 2\pi\delta(x)\vec{S}$ (see Eq. (14) of paper III). Thus, in the combination $H - Y$ that occurs in the density matrix ρ , eV simply plays the role of a *bulk* magnetic field in the z -direction, which can be gauged away exactly by a gauge transformation^{25,eq. (3.37)}. Hence in this model, non-equilibrium properties can be calculated exactly using CFT.

³⁶It is easy to check that the operator J_{eo} is indeed allowed at the boundary: it must be the product $\Phi_e \Phi_o$ of boundary operators in the even and odd sectors, with quantum numbers $(Q_e, j_e, f_e) = (-Q_o, j_o, f_o) = (\pm 1, \frac{1}{2}, \frac{1}{2})$. Φ_o , which lives on a free boundary (since the odd sector is free), is simply the free fermion field $\psi_{o\alpha i}$ in the odd sector. Φ_e must live on a Kondo boundary, which indeed does allow a boundary operators with the quantum quantum numbers $(\pm 1, \frac{1}{2}, \frac{1}{2})$, as may be checked by AL’s double fusion procedure (see table 1c of¹¹).

³⁷See, for example,⁷¹. At $T = 0$, one can prove that δS_V generates such a rotation by closing the $\int_{-\infty}^{\infty} d\tau$ integral along an infinite semi-circle in the lower half-plane (this is allowed, because $J_{eo}(z) \sim z^{-2} \rightarrow 0$ along such a contour^{72,Eq.(2.19)}); having closed the contour, δS_V has precisely the form required for a generator of e/o rotations.

$$\overline{R}_{\bar{\eta}\bar{\eta}'}(V) = \delta_{\bar{\alpha}\bar{\alpha}'}\delta_{\bar{i}\bar{i}'} \begin{pmatrix} \cos\theta_V & -i\sin\theta_V \\ -i\sin\theta_V & \cos\theta_V \end{pmatrix}_{\bar{\sigma}\bar{\sigma}'} , \quad \text{where } \theta_V \equiv \arctan\left(\frac{cV}{T_K}\right) . \quad (I4)$$

Here θ_V is simply a convenient way to parametrize the rotation⁷¹. Thus, the effect of δS_V can be incorporated by replacing the scattering amplitude $\tilde{U}_{\bar{\eta}\bar{\eta}'}(\varepsilon)$ of Eq. (46) by $\overline{R}_{\bar{\eta}\bar{\eta}''}(V)\tilde{U}_{\bar{\eta}''\bar{\eta}'}(\varepsilon)$. Evidently, the final scattering amplitude $\tilde{U}_{\bar{\eta}\eta}(\varepsilon)$ of Eq. (45) will now be V -dependent.

It turns out that for the simple form (9) used for the backscattering matrix $V_{\sigma\sigma'}$, this extra V -dependence “accidentally” cancels out³⁸ in Eq. (51) for $P_\eta(\varepsilon)$. However, for more general forms of $V_{\sigma\sigma'}$, it survives. To lowest order in V/T_K , there will then be a contribution to the conductance of the form $(V/T_K)T^{1/2}\Gamma_1(V/T) = T^{3/2}\Gamma_2(V/T)$. However, this is evidently only a *subleading* correction to the scaling function of Eq. (58). It is of the same order as corrections arising from subleading irrelevant operators of the equilibrium theory, that we have argued in section V 3 would not be worth while calculating since there are too many independent ones.

To summarize the results of this appendix: when $V \neq 0$, corrections to the scattering amplitudes $\tilde{U}_{\eta\eta'}(\varepsilon')$ of order V/T_K can arise; however, they only give rise to *subleading* corrections to the scaling function $\Gamma(v)$.

³⁸This can be seen from by replacing \overline{U} by $\overline{R}\overline{U}$ in Eq. (51) for $P_\eta(\varepsilon)$, and checking that $\overline{R}^\dagger N\sigma^z N^\dagger \overline{R} = \overline{R}^\dagger \sigma^x \overline{R} = \sigma^x$, which is independent of V because \overline{R} generates rotations around the x -axis in the e/o indices. However, if V and N are more complicated than in Eqs. (9) and (11), the V -dependence will clearly not cancel out.

REFERENCES

* Present Address: Institut für Theoretische Festkörperphysik, Universität Karlsruhe, D-76128 Karlsruhe, Germany

¹ JAN VON DELFT, D. C. RALPH, R. A. BUHRMAN, A. W. W. Ludwig and V. Ambegaokar, submitted to Annals of Physics.

² JAN VON DELFT, A. W. W. LUDWIG AND V. AMBEGAOKAR, present paper.

³ JAN VON DELFT AND A. W. W. LUDWIG, submitted to Annals of Physics.

⁴ D. C. RALPH AND R. A. BUHRMAN, Phys. Rev. Lett. **69**, 2118 (1992).

⁵ D. C. RALPH, Ph.D. dissertation, Cornell University (1993).

⁶ D. C. RALPH, A. W. W. LUDWIG, J. von DELFT, AND R. A. BUHRMAN, Phys. Rev. Lett. **72**, 1064 (1994).

⁷ D. C. RALPH AND R. A. BUHRMAN, Phys. Rev. B **51**, 3554 (1995).

⁸ A. ZAWADOWSKI, Phys. Rev. Lett. **45**, 211 (1980).

⁹ K. VLADÁR AND A. ZAWADOWSKI, Phys. Rev. B **28**, (a) 1564; (b) 1582; (c) 1596 (1983).

¹⁰ I. AFFLECK AND A. W. W. LUDWIG, Phys. Rev. B **48**, 7297 (1993).

¹¹ A. W. W. LUDWIG, Int. Jour. Mod. Phys. **B8**, 347 (1994).

¹² (a) N. S. WINGREEN, B. L. ALTSCHULER AND Y. MEIR, Phys. Rev. Lett. **75**, 770 (1995);
(b) D. C. RALPH, A. W. W. LUDWIG, J. von DELFT, AND R. A. BUHRMAN, Phys. Rev. Lett. **75**, 771 (1995); **75**, 2786(E) (1995).

¹³ M. H. HETTLER, J. KROHA, AND S. HERSHFIELD, Phys. Rev. Lett. **73**, 1967 (1994).

¹⁴ SELMAN HERSHFIELD, Phys. Rev. Lett., **70**, 2134 (1993).

¹⁵ A. L. MOUSTAKAS AND D. S. FISHER, **53**, 4300 (1996); see also Phys. Rev. B **51**, 6908 (1995).

¹⁶ G. ZARÁND AND A. ZAWADOWSKI, Physica B 218, 60 (1996).

¹⁷ A. ZAWADOWSKI, G. ZARÁND, NOZIÈRES, VLADÁR AND G. ZIMÁNYI, preprint (1997).

¹⁸ L. P. KADANOFF AND G. BAYM, *Quantum Statistical Mechanics*, Benjamin, New York (1962).

¹⁹ G. ZARÁND AND L. UDVARDI, Phys. Rev. B, **54**, 7606 (1996).

²⁰ A. G. M. JANSEN, A. P. VAN GELDER AND P. WYDER, J. Phys. C. **13**, 6073 (1980).

²¹ E. MERZBACHER, *Quantum Mechanics*, 2nd. Ed., John Wiley & Sons (1970).

²² J. M. Maldacena AND A. W. W. LUDWIG, preprint con-mat/9502109 (1995).

²³ I. AFFLECK, Nucl. Phys. **B336**, 517 (1990).

²⁴ I. AFFLECK AND A. W. W. LUDWIG, Nucl. Phys. **B352**, 849 (1991).

²⁵ I. AFFLECK AND A. W. W. LUDWIG, Nucl. Phys. **B360**, 641 (1991).

²⁶ I. AFFLECK, A. W. W. LUDWIG, H.-B. PANG AND D. L. COX, Phys. Rev. **B45**, 7918 (1992).

²⁷ I. AFFLECK AND A. W. W. LUDWIG, Nucl. Phys. **B428**, 545 (1994).

²⁸ V. AMBEGAOKAR, "The Green's Function Method", in *Superconductivity*, ed. R. D. Parks, Marcell Dekker (1969).

²⁹ A. SCHILLER AND S. HERSHFIELD, Phys. Rev. B **51**, 12896 (1995). We thank these authors for showing us their results prior to publication.

³⁰ M. H. HETTLER, J. KROHA, AND S. HERSHFIELD, to be published. We thank these authors for their kind permission to included not yet published results of theirs in our paper.

³¹ D. L. COX AND A. E. RUCKENSTEIN, Phys. Rev. Lett. **71**, 1613 (1993).

³² I. O. KULIK, R. I. SHEKHTER AND A. N. OMELYANCHOUK, Solid State Comm. **23**, 301 (1977).

³³ A. N. OMELYANCHUK, I. O. KULIK AND R. I. SHEKHTER, Pis'ma Zh. eksp. Teor. Fiz. **25**, 465 (1977) [JETP Lett., **25**, 437 (1977)].

³⁴ I. O. KULIK, A. N. OMELYANCHOUK AND R. I. SHEKHTER, Fiz. Nizk. Temp. **3**, 1543 (1977) [Sov. J. Low. Temp. Phys. **3**, 740 (1977)].

³⁵ A. M. DUIF, A. G. JANSEN AND P. WYDER, J. Phys.: Cond. Matt. **1**, 3157 (1989).

³⁶ J. L. BLACK, K. VLADÁR AND A. ZAWADOWSKI, Phys. Rev. B **26**, 1559 (1982).

³⁷ K. VLADÁR AND G. T. ZIMÁNYI, J. Phys. C **18**, 3755 (1985).

³⁸ K. VLADÁR, G. T. ZIMÁNYI AND A. ZAWADOWSKI, Phys. Rev. B **56** 286 (1986).

³⁹ K. VLADÁR, A. ZAWADOWSKI AND G. T. ZIMÁNYI, Phys. Rev. B **37**, 2001, 2015 (1988).

⁴⁰ G. ZARÁND, Solid St. Comm. **86**, 413 (1993).

⁴¹ G. ZARÁND AND A. ZAWADOWSKI, Phys. Rev. Lett. **72**, 542 (1994).

⁴² G. ZARÁND AND A. ZAWADOWSKI, Phys. Rev. B **50**, 932 (1994).

⁴³ G. ZARÁND, Phys. Rev. B **51**, 273 (1995).

⁴⁴ A. ZAWADOWSKI AND K. VLADÁR, in *Quantum Tunneling in Condensed Media*, ed. Yu. Kagan and A. J. Leggett (Elsevier, 1992) p. 427.

⁴⁵ D. L. COX AND A. ZAWADOWSKI, Review Article: "Exotic Kondo Effects in Real Materials", to be published (1995).

⁴⁶ C. C. YU AND P. W. ANDERSON, Phys. Rev. B **29**, 6165 (1984).

⁴⁷ V. HAKIM, A. MURAMATSU AND F. GUINEA, Phys. Rev. B **30**, 464 (1984); A. J. LEGGETT *et al.*, Rev. Mod. Phys. **59**, 1 (1987).

⁴⁸ A. MURAMATSU AND F. GUINEA, Phys. Rev. Lett. **57**, 2337 (1986).

⁴⁹ P. W. ANDERSON, J. Phys. C., **3**, 2436 (1970), P. W. ANDERSON AND G. YUVAL, *Magnetism*, Vol. **5**, Chapter 7, G.T. RADO AND H. SUHL, eds. Academic Press, New York, (1973).

⁵⁰ G. ZARÁND AND K. VLADÁR, Phys. Rev. Lett. **76**, 2133 (1996).

⁵¹ K. G. WILSON, Rev. Mod. Phys., **47**, 773 (1975).

⁵² H. R. KRISHNAMURTHY, H.R. WILKINS, K. G. WILSON, Phys. Rev. B**21**, 1003 & 1044, (1980).

⁵³ D. M. CRAGG, P. LLOYD AND P. NOZIÈRES, J. Phys. **13**, 245 (1980).

⁵⁴ H.-B. PANG, Ph.D. dissertation, The Ohio State University, unpublished (1992); H.-B. PANG AND D. L. COX, Phys. Rev. B **44**, 9454 (1991).

⁵⁵ A. C. HEWSON, *The Kondo Problem to Heavy Fermions*, Cambridge University Press, 1993.

⁵⁶ W. KOHN AND S. H. VOSKO, Phys. Rev. **119**, 912 (1960).

⁵⁷ D. L. COX, private communication.

⁵⁸ G. ZARÁND, Phys. Rev. Lett., **77**, 3609 (1996).

⁵⁹ J.E. GRAEBNER, B. GOLDING, R. J. SCHUTZ, F. S. L. HSU AND H. S. CHEN, Phys. Rev. Lett. **39**, 1480 (1977).

⁶⁰ G. GOLDING, N. M. ZIMMERMAN, S. N. COPPERSMITH, Phys. Rev. Lett. **68**, (1992).

⁶¹ N. W. ZIMMERMAN, B. GOLDING, W. H. HAEMMERLE, Phys. Rev. Lett. **67**, 1322 (1991).

⁶² C. DOBLER AND JAN VON DELFT, work in progress.

⁶³ J. KONDO, Prog. Theor. Phys. **32**, 37 (1964).

⁶⁴ J.-W. GAN, J. Phys. Condens. Matter, **6**, 4547 (1994).

⁶⁵ L. V. KELDYSH, Zh. Eksp. Teor. Fiz. **47**, 1515 (1964) [Sov. Phys. JETP **20**, 1018 (1965)].

⁶⁶ J. RAMMER AND H. SMITH, Rev. Mod. Phys. **58**, 323 (1986).

⁶⁷ N. E. BICKERS, Rev. Mod. Phys. **59**, 845 (1987).

⁶⁸ N. S. WINGREEN AND Y. MEIR, Phys. Rev. B, **49**, 11040 (1994).

⁶⁹ Y. MEIR, N. S. WINGREEN AND P. A. LEE, Phys. Rev. Lett. **70**, 2601 (1993).

⁷⁰ A. SCHILLER AND S. HERSHFIELD, private communication.

⁷¹ C. G. CALLAN, I. G. KLEBANOV, A. W. W. LUDWIG AND J. M. MALDACENA, Nucl. Phys. **B422**, 417 (1994).

⁷² V. G. KNIZHNIK AND A. B. ZAMOLODCHIKOV, Nucl. Phys. **B247**, 83 (1984).

FIGURES

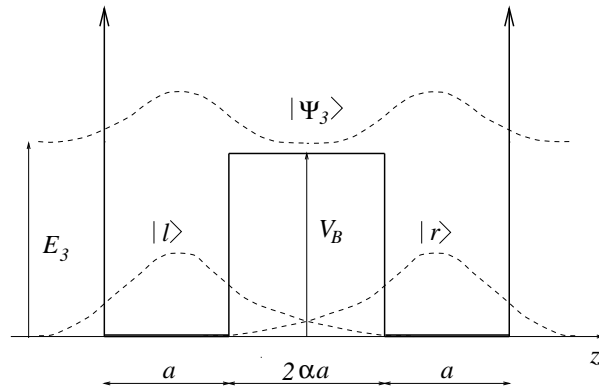


FIG. 1. A symmetrical square double well potential (heavy line), such as that used by Zaránd and Zawadowski for their model calculations, and the wave-functions for the states $|r\rangle$, $|l\rangle$ and the first excited state $|\Psi_3\rangle$.

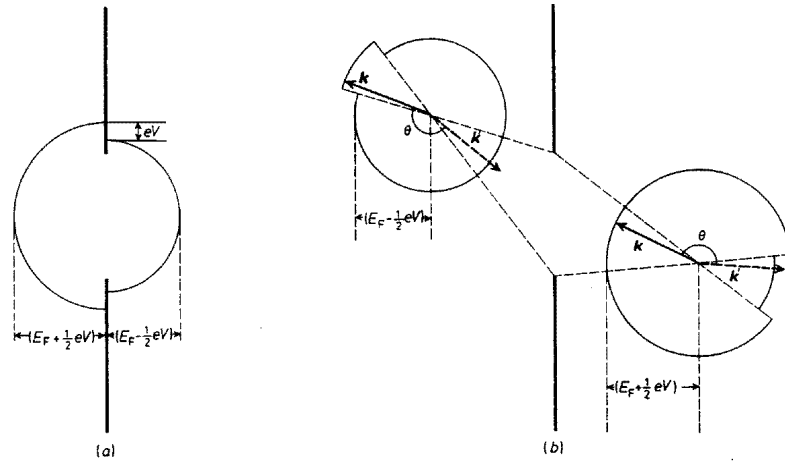


FIG. 2. (taken from^{20, Fig. 7}): The $T = 0$ electron distribution function $f_{\vec{k}}^{(0)}(\vec{r})$ shown (a) at the hole and (b) at two points near the hole. The picture is a position-momentum space hybrid, showing the momentum-space distribution function $f_{\vec{k}}^{(0)}$ with its origin drawn at the position \vec{r} to which it corresponds. A finite temperature simply smears out the edges of the two (R/L) Fermi seas.

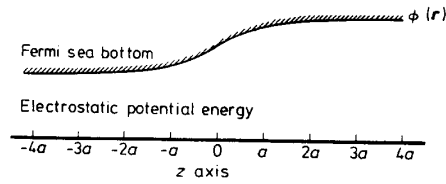


FIG. 3. (taken from^{20, Fig. 6}): The electrostatic potential energy $e\phi^{(0)}(\vec{r})$, which defines the bottom of the conduction band, near a point contact with radius a , shown along the z -axis for the case $eV > 0$. Within a few radii a from the hole, $e\phi^{(0)}(\vec{r})$ changes smoothly from $-eV/2$ on the left to $+eV/2$ on the right.

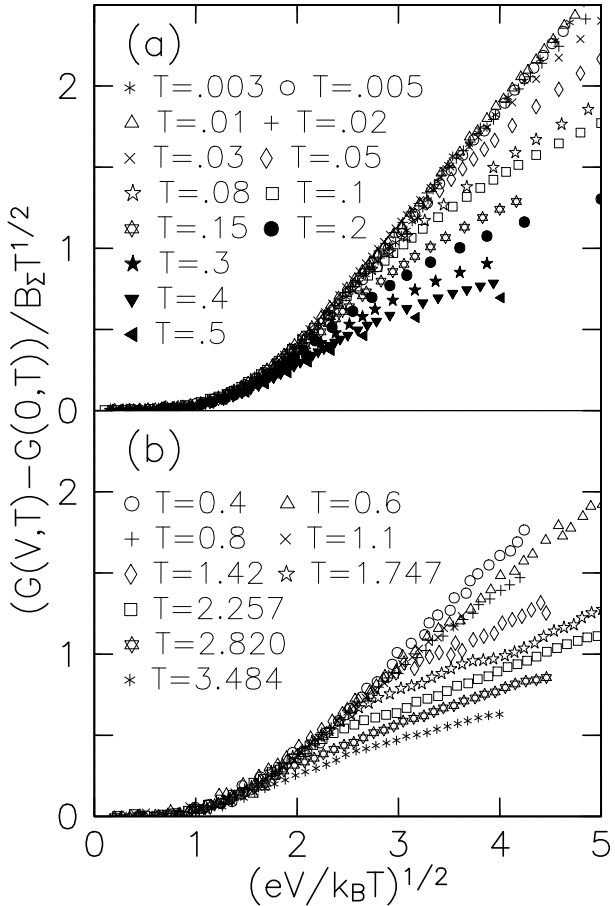


FIG. 4. Scaling plots of the conductance for (a) the NCA calculations of Hettler *et al.*¹³ and (b) experiment (sample #1). With B_Σ determined from the zero-bias conductance, $G(0, T) = G(0, 0) + B_\Sigma T^{1/2}$, [Eq. (23)], there are no adjustable parameters. The temperatures in the NCA- and experimental plots are in units of T_K and Kelvin, respectively.

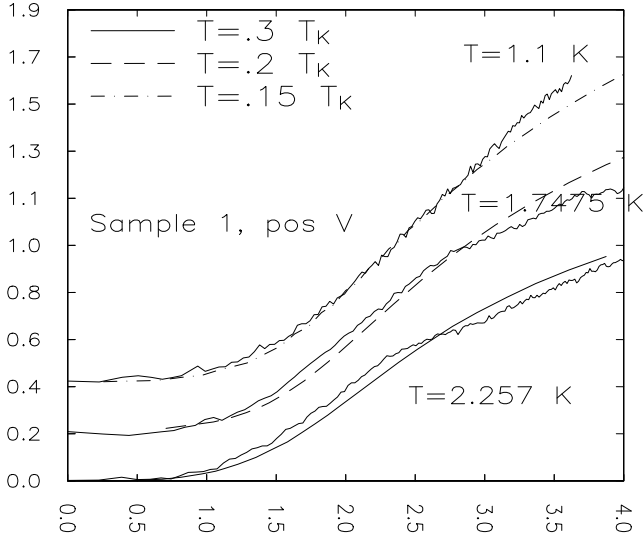


FIG. 5. Comparison between NCA theory and experiment for three individual conductance curves from sample # 1. By using T_K as a single fitting parameter and choosing $T_K = 8K$ for sample 1, this kind of agreement is achieved simultaneously for a significant number of individual curves [Hettler, private communication],³⁰. The NCA curves shown here correspond to $T = 0.3T_K = 2.4K$, $0.2T_K = 1.6K$ and $0.15T_K = 1.2K$ (NCA curves for the actual experimental temperatures of $T = 2.257K$, $1.745K$ and $1.1K$ were not calculated.)

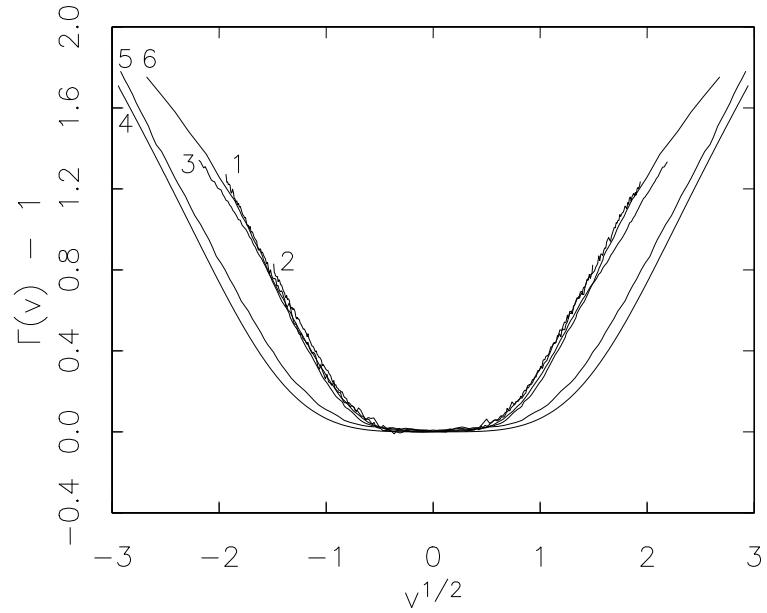


FIG. 6. The conductance scaling function $\Gamma(v)$. Curves 1,2,3 are the experimental curves of Fig. 11 (b). Curve 4 is the CFT prediction from Eq. (56). Curves 5 and 6 are the NCA results of HKH, with $T/T_K = 0.003$ and 0.08 , respectively. All curves have been rescaled in accordance with Eq. (56).

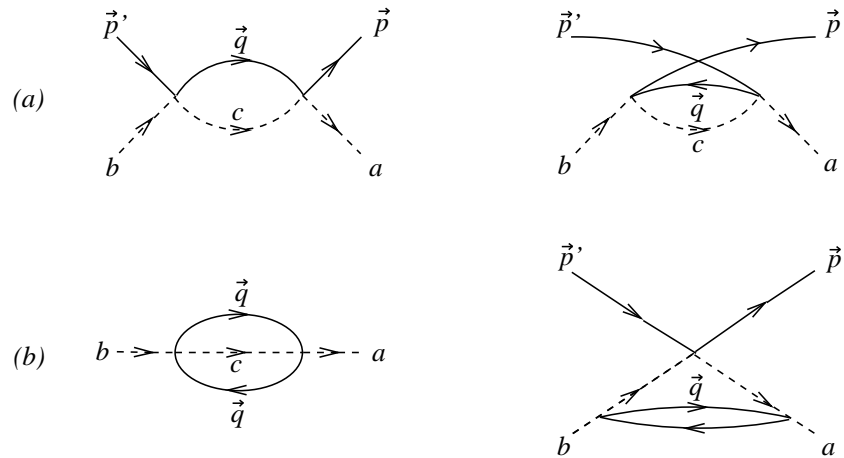


FIG. 7. (a) The second-order vertex corrections that contribute to Eq. (B8) and generate the leading order scaling equation (C3). (b) The impurity self-energy correction and the third-order next-to-leading-logarithmic vertex correction that generate the subleading terms in the second-order scaling equation (C9). (Note that subleading diagrams that are generated by the leading-order scaling relation derived from the diagrams in (a) have to be omitted.) Dashed and solid lines denote impurity and electron Green's functions, respectively.

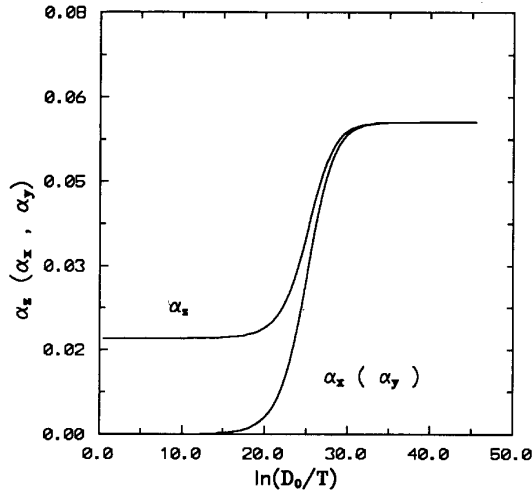


FIG. 8. Scaling trajectories of the matrix norms $\alpha^A \equiv \text{Tr}[(\underline{y}^A)^2]$ ($A = x, y, z$), calculated numerically for the case $N_f = 3$. All three norms tend to the same value, in accord with eq. (C12). Consult⁴³, from which this figure was taken, for details regarding the initial parameters used.

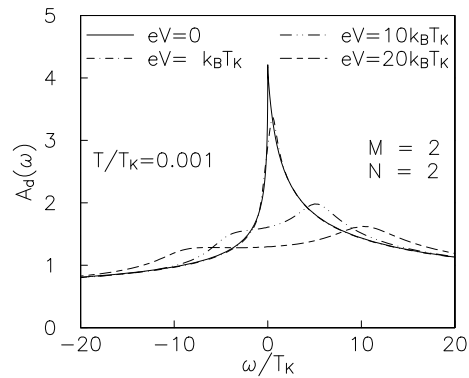


FIG. 9. The Kondo resonance in the impurity spectral function $A_d(\omega)$, calculated $T/T_K = 0.001$ using the NCA³⁰. For our purposes the most important feature of this figure is that the Kondo peak does not start to split for $eV < T_K$.